Running head: Role of cyanide in plant immune response

Correspondence: Irene García. Instituto de Bioquímica Vegetal y Fotosíntesis. Centro de Investigaciones Científicas Isla de la Cartuja, CSIC and Universidad de Sevilla, Avenida Américo Vespucio, 49, 41092 Sevilla, Spain. Tel: 34.954489578. Fax: 34.954461065. Email: irene.garcia@ibvf.csic.es

Journal research area: Signaling and Response

Transient transcriptional regulation of the *CYS-C1* gene and cyanide accumulation upon pathogen infection in the plant immune response

Irene García[1,*], Tábata Rosas[2], Eduardo R. Bejarano[2], Cecilia Gotor[1] and Luis C. Romero[1]

[1]Instituto de Bioquímica Vegetal y Fotosíntesis, Consejo Superior de Investigaciones Científicas and Universidad de Sevilla, Avenida Américo Vespucio 49, E-41092 Sevilla, Spain

Instituto de Hortofruticultura Subtropical y Mediterránea "La Mayora" (IHSM-UMA-CSIC), Departamento de Genética, Facultad de Ciencias, Universidad de Málaga, Campus de Teatinos s/n, E-29071 Málaga, Spain.

Summary: The analysis of a mutant in the main enzyme responsible for cyanide detoxification, the mitochondrial ß-cyanoalanine synthase, uncovers a new signaling role for cyanide in the plant response to pathogens

This work was funded by the European Regional Development Fund (ERDF) through the Ministerio de Economía y Competitividad (grant no. BIO2010-15201 and CSD2007–00057) and by the Junta de Andalucía, Spain (grant no. CVI-7190)

*Corresponding author: Irene García. E-mail: irene.garcia@ibvf.csic.es

ABSTRACT

Cyanide is produced concomitantly with ethylene biosynthesis. *Arabidopsis thaliana* detoxify cyanide primarily through the enzyme ß-cyanoalanine synthase (CAS), mainly by the mitochondrial CYS-C1. The *CYS-C1* loss-of-function is not toxic for the plant and it leads to an increased level of cyanide in *cys-c1* mutants as well as a root hairless phenotype. The classification of genes differentially expressed in *cys-c1* and wild type plants reveals that the high endogenous cyanide content of the *cys-c1* mutant is correlated with the biotic stress response. Cyanide accumulation and *CYS-C1* gene expression are negatively correlated during compatible and incompatible plant-bacteria interactions. In addition, *cys-c1* plants present an increased susceptibility to the necrotrophic fungus *Botrytis cinerea* and an increased tolerance to the biotrophic *Pseudomonas syringae* pv. *tomato DC3000* bacterium and *Beet curly top virus*. *cys-c1* mutation produces a reduction in respiration rate in leaves, an accumulation of reactive oxygen species and an induction of the alternative oxidase *AOX1a* and the pathogenesis-related *PR1* expression. We hypothesize that cyanide, which is transiently accumulated during avirulent bacterial infection and constitutively accumulated in *cys-c1* mutant, uncouples the respiratory electron chain dependent on the cytochrome c oxidase, and this uncoupling induces the alternative oxidase activity and the accumulation of reactive oxygen species, which act by stimulating the salicylic acid-dependent signaling pathway of the plant immune system.

Key words: *Arabidopsis thaliana*, cyanide, ß-cyanoalanine synthase, plant immune response, *Pseudomonas syringae*, *Botrytis cinerea*, *Beet curly top virus*, reactive oxygen species, mitochondrial respiratory chain

INTRODUCTION

The gaseous hormone ethylene is known to regulate multiple physiological and developmental processes in plants, such as seedling emergence, leaf and flower senescence, climacteric fruit ripening and organ abscission. Ethylene is also involved in the response of plants to abiotic and biotic stresses (Wang et al., 2002; Broekaert et al., 2006; van Loon et al., 2006). Enhanced ethylene production is an early, active response of plants to the perception of pathogen attack and is associated with the induction of defense reactions. During ethylene biosynthesis, S-adenosyl-L-methionine (AdoMet) is converted to 1-aminocyclopropane-1-carboxylic acid (ACC) by ACC synthase (ACS). ACC is finally oxidized by ACC oxidase (ACO) to form ethylene, carbon dioxide and cyanide (Hartley et al., 1998; Wang et al., 2002) Hydrogen cyanide (HCN) is a colorless and highly volatile liquid. The anion cyanide (CN^-) is toxic and renders the cells of an organism unable to use oxygen, primarily through the chelation of di- and trivalent metal ions in the prosthetic groups of several metalloenzymes, including Cu/Zn superoxide dismutase, catalase, nitrate and nitrite reductase, nitrogenase, peroxidases and the mitochondrial cytochrome c oxidase (Isom and Way, 1984; Donato et al., 2007).

Cyanide must be rapidly detoxified and metabolized by the plant to keep the concentration below toxic levels. Plants detoxify cyanide primarily through the enzyme ß-cyanoalanine synthase (CAS), for which considerable levels of activity are constitutively found in many plant species. Rhodanese and mercaptopyruvate sulfurtransferase activity also make minor contributions to the cyanide detoxification process (Miller and Conn, 1980). ß-cyanoalanine synthase is a pyridoxal phosphate-dependent enzyme that converts Cys and cyanide to hydrogen sulfide and ß-cyanoalanine, which are later converted to Asn, Asp and ammonia by NIT4 class nitrilases (Piotrowski, 2008). Arabidopsis plants carry the mitochondrial ß-cyanoalanine synthase CYS-C1 (At3g61440) (Watanabe et al., 2008), which belongs to the family of ß-substituted alanine synthase enzymes. The family also includes the three major O-acetylserine(thiol)lyase enzymes OAS-A1 (At4g14880), OAS-B (At2g43750) and OAS-C (At3g59760) (Watanabe et al., 2008); the L-cysteine desulfhydrase DES1 (At5g28030) (Alvarez et al., 2010); the S-sulfocysteine synthase CS26 (At3g03630) (Bermudez et al., 2010); and the functionally unknown cytosolic isoforms CYS-D1 (At3g04940) and CYS-D2

(At5g28020). Mutations in CYS-C1 result in plants that accumulate cyanide and that display abnormal root hair (Garcia et al., 2010), suggesting that cyanide has a signaling role in root development. The lack of the mitochondrial OASTL isoform OAS-C, which is necessary to detoxify the sulfide released by the CAS activity, causes an accumulation of sulfide and cyanide and a root phenotype similar to the *cys-c1* loss-of-function mutant (Álvarez et al., 2012b).

Several authors have suggested that cyanide could act as a regulator of other metabolic processes in addition to performing the described role in plant root development (Siegien and Bogatek, 2006). It has been observed that this molecule is released during seed germination and that exogenously applied HCN breaks seed dormancy in several plants (Cohn and Hughes, 1986; Fol et al., 1989; Bogatek et al., 1991; Bethke et al., 2006). The role of cyanide as a regulatory molecule is not restricted to plants, and it has been demonstrated that cyanide is generated in leukocytes from glycine via a peroxidase (Stelmaszynska, 1986) as well as in the central nervous system, where it has been hypothesized to act as a neuromodulator (Gunasekar et al., 2000; Cipollone and Visca, 2007). Cyanide production can be stimulated by opiates and decreased by treatment with muscarinic receptor agonists (Borowitz et al., 1997; Gunasekar et al., 2004).

Despite the variety of known functions for cyanide in different organisms, the role of cyanide production in plants seems to have been unevaluated to date. In cyanogenic plants, cyanide is produced during the degradation of cyanogenic lipids and from the catabolism of cyanogenic glycosides (Poulton, 1990). Cyanide and cyanogenic compounds play an important role in plant defense against herbivores (Zagrobelny et al., 2008). In non-cyanogenic plants, cyanide is a co-product of ethylene biosynthesis. The molecule is also produced during the biosynthesis of camalexin, a phytoalexin formed in Arabidopsis plants upon infection by a large variety of microorganisms, including bacteria, fungi and oomycetes (Glawischnig, 2007). During camalexin biosynthesis, the tryptophan-derived intermediate indole-3-acetonitrile is conjugated with cysteine and serves as a substrate for the cytochrome P450 enzyme CYP71B15. This enzyme catalyzes the formation of the thiazoline ring as well as the release of cyanide and subsequent oxidative decarboxylation of dihydrocamalexic acid to camalexin (Glawischnig, 2007; Bottcher et al., 2009). Since both cyanide sources, camalexin and ethylene, are produced after pathogen attack, cyanide should be produced at

significant levels during plant response to pathogens. It has been shown that exogenous cyanide can enhance the resistance of tobacco and Arabidopsis leaves to *Tobacco mosaic virus* and *Turnip vein clearing virus*, respectively (Chivasa and Carr, 1998; Wong et al., 2002). Recently, it has been demonstrated that exogenously applied cyanide increases the resistance of young rice plants to blast fungus infection, suggesting that cyanide rather than ethylene contributes to plant resistance (Seo et al., 2011).

This work aims to further investigate the role of endogenously produced cyanide in the plant immune response by analyzing the behavior of Arabidopsis knockout mutants of the mitochondrial ß-cyanoalanine synthase CYS-C1 and the regulation of CYS-C1 in response to pathogen attack.

RESULTS

cys-c1 Mutant Transcriptome Shows a High Correlation with Biotic Stresses

The loss of function of the CYS-C1 enzyme has previously been characterized in root tissues, but its function in leaves has not been studied to date (García et al 2010). Phenotypic analysis of the *cys-c1* null mutant shows no obvious alterations in the aerial parts of the plant whether grown in long- or short-day photoperiods. To analyze the effect of the loss of function of the CYS-C1 enzyme at the molecular level, we performed a comparative transcriptomic analysis of leaves of *cys-c1* and wild type plants grown under identical long-day conditions on MS medium for 14 days. Total RNA was prepared and analyzed using the Affymetrix-Arabidopsis ATH1GeneChip array. Three biological replicates were performed for each genotype. Restricting the analysis to the genes whose expression was changed at least 2-fold as a threshold and at a significance level of $P < 0.05$, we identified 51 genes that exhibited alterations in transcription level. Among them, 31 genes were up-regulated in the *cys-c1* mutant plant compared with the wild type plant, and 20 genes were down-regulated (Microarray Gene Expression Omnibus database accession number GSE19242, Table S1). To detect physiologically relevant patterns, the genes with altered expression were assigned to functional categories based on classification by the Bio-Array Resource for Arabidopsis Functional Genomics, BAR (Toufighi et al., 2005). The resulting group lists revealed that a high proportion of both up- and down- regulated genes in the *cys-c1* mutant were associated with the plant's responses to biotic and abiotic stress and signaling (Supplemental Fig. S1). The induction of selected genes such as *WRKY33* (encoding a WRKY transcription factor), *ERF6* (encoding a ethylene response transcription factor), *CYP81F2* (encoding a cytochrome P450 involved in glucosinolate biosynthesis) and *GSTU24* (coding for a putative glutathione-S-transferase) was confirmed by real-time RT-PCR, thus validating the data obtained by the array (Supplemental Fig. S2)

A meta-analysis of the *cys-c1* transcript profile data was performed by comparison with the available Affymetrix-Arabidopsis ATH1GeneChip array databases and use of the analytical tools of Genevestigator (Hruz et al., 2008). Biclustering and hierarchical clustering analysis of the up- and down-regulated genes in *cys-c1* showed that 80% were co-regulated with genes

that were de-regulated in wild type seeds of the ecotype Col-0 after treatment with 0.1% oxygen for six days (GSE14420) (Christianson et al., 2009) (Supplemental Fig. S3 and Table S2). In comparing microarray data for the gene subset categorized as biotic, 54% of the genes identified overlapped with those already shown to be affected by fungal pathogens or altered in *Pseudomonas syringae* pv. *tomato*-infected Arabidopsis plants or elicitor-treated plants (Supplemental Fig. S4, S5 and Table S2). Among the genes identified in these groups are several transcription factors related to biotic defense response, such as WRKY18, WRKY33, WRKY40 and the gene coding for FLG22-INDUCED RECEPTOR-LIKE KINASE 1 (FRK1, AT2G19190). No correlation was found with ACC treatments or mutants in the ethylene signaling (Supplemental Fig. S6).

In the light of this analysis, it is interesting to speculate that cyanide plays a role in signaling and defense against pathogen infection in leaf tissues. We aimed then to investigate this hypothesis further.

Cyanide Accumulates during the Infection of Arabidopsis Plants with *Botrytis cinerea*

Botrytis cinerea is a necrotrophic pathogen that causes gray mold diseases in many crop plants, resulting in significant crop losses. *Botrytis* and other necrotrophic pathogens promote and benefit from host cell death during pathogenesis, as dead cells and necrotic tissues provide a base for saprophytic growth from which *Botrytis* further colonizes healthy tissue (AbuQamar et al., 2006). When plants are infected by *B. cinerea*, they produce high levels of ethylene (Cristescu et al., 2002; Han et al., 2010). Figure 1A shows that the ethylene production increases rapidly in *A. thaliana* when challenged with *B. cinerea*, reaching a maximum level at 24 hours post-infection (hpi). We investigated the accumulation of the cyanide coproduced during the *B. cinerea-A. thaliana* interaction as well as the regulation of the *CYS-C1* gene under these conditions. At the beginning of the interaction, the level of cyanide dropped transiently at 9 hpi and then started accumulating, reaching a maximum of 190% of the basal level at 15 hpi (Fig. 1B); accordingly, *CYS-C1* expression shows a waving curve with expression peaks at 3 hpi and 24 hpi and a valley at 15 hpi, this last level coinciding with the higher level of cyanide (Fig. 1C).

Cyanide Accumulation and *CYS-C1* Gene Expression are Negatively Correlated during Compatible and Incompatible Plant-Bacteria Interactions

The bacterial pathogen *Pseudomonas syringae* is a hemibiotrophic pathogen that produces bacterial specks in a wide range of plant species. In the early stages of compatible infections, host cell death does not occur. Later stages of infection, however, are associated with host tissue chlorosis and necrosis (Glazebrook, 2005).

Besides the non-host resistance, plants have the capacity to recognize pathogen associated molecular patterns (PAMPs) by surface pattern-recognition receptors (PRRs) and to induce a response leading to a basal or PAMP-triggered immunity (PTI) (Jones and Dangl, 2006). Some pathogens have evolved to avoid recognition by delivering effectors that suppress PTI and this results in a compatible plant-pathogen interaction. For their defense, plants have also evolved resistance (*R*) genes that encode receptors recognizing specific pathogen effectors, resulting in effector-triggered immunity (ETI) (Jones and Dangl, 2006). In addition to the PTI response, *P. syringae pv. tomato (Pst) DC3000* can elicit an ETI reaction in Arabidopsis when expressing the type III effector AvrRpm1 (Bent et al., 1994; Mindrinos et al., 1994; Grant et al., 1995). When tobacco plants are infected by *P. syringae*, they produce ethylene. The production is monophasic if the bacteria do not elicit an HR and produce a disease and biphasic if the bacteria induce an HR and do not subsequently produce a disease (Mur et al., 2008). Moreover, transcriptomic data suggest that genes encoding ethylene biosynthetic enzymes were upregulated in Arabidopsis following challenge with avirulent bacteria (Mur et al., 2008). To investigate this response further, the production of ethylene was monitored during a compatible and an incompatible interaction. Arabidopsis plants were infected with a virulent *Pst DC3000* or an avirulent *Pst DC3000 avrRpm1* strain. Samples were taken at 1, 3, 6, 9 and 24 hpi. Ethylene was accumulated in the early stages of both interactions, although the accumulation occurred earlier in the incompatible interaction than in the compatible interaction. A second rise occurred at 9 hpi of the avirulent interaction (Fig. 2A). The infection with *Pst DC3000* induced ethylene accumulation only at the very late stages of the interaction (24 hpi). These data are in agreement with the results already published for the tobacco-*Pseudomonas* interaction (Mur et al., 2008).

We also determined the kinetics of the accumulation of cyanide in the same samples. Interestingly, cyanide accumulated at different rates in the two *Arabidopsis-Pst* interactions, being detoxified preferentially during the compatible interaction (Fig. 2B). In fact, during ETI, cyanide started accumulating at 3 hpi, and its level did not decrease significantly during the infection. In contrast, during the PTI, cyanide content decreased at 1 hpi, increased to the basal level at 3 and 6 hpi, then decreased and started increasing again after 9 hpi to reach the basal level of 24 hpi. Accordingly, the transcription of *CYS-C1* was induced during the compatible interaction and was repressed during the ETI, with the curve showing an opposite peak at 3 hpi (Fig. 2C).

Mitochondrial Cyanide Differentially Affects the Response to a Necrotrophic and a Biotrophic Pathogen, and This Effect Is Reversed with Hydroxocobalamin Treatment

Non-lethal concentrations of cyanide can enhance the resistance of plants to fungi (Seo et al., 2011). *cys-c1* mutant plants have been shown to accumulate more cyanide in both root and leaf tissues and to exhibit less ethylene accumulation than wild type plants (García et al., 2010). To investigate the possible role of mitochondrial cyanide in plant defense against pathogens, *cys-c1* mutant plants defective in the mitochondrial CAS (Garcia et al., 2010) were challenged by a necrotrophic (*B. cinerea*) and a hemibiotrophic (*P. syringae pv. tomato* DC3000 -*Pst DC3000*-) compatible pathogen. When challenged with the fungus, *cys-c1* showed more severe symptoms than wild type plants and accumulated 6 times more *B. cinerea* DNA (Fig. 3A-B). Conversely, the *cys-c1* mutant exhibited a higher tolerance to the infection by *Pst DC3000* than the Col-0 wild type, as it showed less severe symptoms than wild type plants and accumulated 12-fold less *Pst DC3000* colony-forming units per mg of fresh weight (cfu mg^{-1}) at 2 day after infection (dpi) than Col-0; the difference was 6-fold at 4 dpi (Fig. 3C-D). However, the susceptibility to an avirulent strain of *Pst DC3000* is not affected by the *cys-c1* mutation (Supplemental Fig. S10).

To confirm that the observed phenotype of the *cys-c1* mutant plants was indeed due to the disruption of the *CYS-C1* gene, complementation analysis was performed using the full-length *CYS-C1* genomic fragment including its promoter region (*Pcys-c1*). *cys-c1* plants transformed

with the *Pcys-c1-CYS-C1* fragment displayed pathogen sensitivity similar to that of the wild type (Supplemental Fig. S11).

Hydroxocobalamin is a natural form of vitamin B12 that is commonly used as an antidote for severe acute cyanide poisoning in humans (Borron et al., 2007; Hall et al., 2007). Hydroxocobalamin can penetrate cells and act at an intracellular level to bind cyanide and form nontoxic cyanocobalamin, which is excreted in the urine (Astier and Baud, 1996). In plants, hydroxocobalamin has been used to antagonize the effect of cyanide in roots, reverting the root hairless phenotype in *cys-c1* lines to that of wild type plants (García et al., 2010). The addition of 10 mM hydroxocobalamin at the time of infection with *Botrytis* reverted the sensitivity phenotype exhibited by the *cys-c1* mutant, decreasing the accumulation of *B. cinerea* DNA in infected *cys-c1* leaves to wild type levels (Fig. 4A). Moreover, this effect was dose dependent, as the treatment with hydroxocobalamin 5 mM partially reverted the susceptibility of the *cys-c1* mutant to *B. cinerea* to levels similar to those of wild type plants (Supplemental Fig. S12). Similarly, the treatment with hydroxocobalamin altered the phenotype of resistance to *Pst DC3000* exhibited by the *cys-c1* mutant, as bacteria were able to develop even better in *cys-c1* plants treated with the antidote than in wild type in either the presence or absence of hydroxocobalamin (Fig. 4B). To exclude the possibility that the hydroxocobalamin directly affected pathogen growth, we performed growth tests of *Pst DC3000* in solid culture LB media in the absence and presence of 5 mM of hydroxocobalamin. No differences were observed in either of the two conditions (Supplemental Fig. S13). Therefore, the possibility of a direct effect of hydroxocobalamin in the pathogen's growth rather than rescuing the *cys-c1* phenotype is excluded.

Mitochondrial Cyanide Is Correlated with Plant Resistance to Viral Pathogens

Non-lethal concentrations of cyanide can enhance the resistance of plants to viral infection (Chivasa and Carr, 1998; Wong et al., 2002). Members of the Geminivirus family are plant viruses with circular, single-stranded DNA genomes (Rojas et al., 2005) that infect a wide range of plant species and that cause extensive losses in crops. To determine whether mitochondrial cyanide accumulation is involved in the cyanide-related resistance to viruses, wild type and *cys-c1* mutant plants were challenged with the geminivirus *Beet curly top virus*

(BCTV). When infected with the virus, *cys-c1* plants exhibited symptoms less severe than those of respective wild type plants (Fig. 5A, B). Plants showing no symptoms (catalogued as 0 by the severity index described in (Baliji et al., 2007)) constituted 26.6% in the case of the *cys-c1* mutant and 5.5 % in the case of the wild type plants. Moreover, the sum of plants showing the category 0 (asymptomatic) plus 1 (mild symptoms) was 40% for the *cys-c1* mutant and only 16.6% for the wild type plants. On the other hand, 33.3% of the *cys-c1* mutant and 61.1% of the wild type plants showed the most severe symptoms, exhibiting almost no plant growth (categorized as 4 in the severity index). When viral DNA present in infected plants was quantified by qPCR, the results clearly showed that the *cys-c1* infected plants accumulated less viral DNA than did wild type plants (Fig. 5C). These results indicate that endogenously produced cyanide can protect plants from virus attack just as exogenously applied cyanide does.

cys-c1 Mutation Produces a Reduction in Respiration Rate in Leaves and an Induction of Alternative Oxidase and _PR1_ Expression

Cyanide binds to the heme iron of the mitochondrial cytochrome c oxidase, thereby blocking the cytochrome respiration pathway and the utilization of oxygen in cellular functions (Donato et al., 2007). In higher plants, an alternative cyanide-resistant respiratory pathway is catalyzed by the alternative oxidase (AOX), which is located in the mitochondrial inner membrane and acts as a terminal oxidase in the mitochondrial electron transport chain. AOX branches from the main respiratory chain at the level of the ubiquinone pool and catalyzes the four-electron reduction of oxygen to water, releasing the energy as heat (Millenaar and Lambers, 2003). Much work has revealed that the genes encoding AOX, AOX protein and the alternative respiratory pathway are frequently induced during plant–pathogen interactions (Hanqing et al., 2010). The *cys-c1* mutant displays a reduction of root (Garcia et al., 2010) and leaf (Fig. 6A) respiration rates. The addition of salicylhydroxamic acid (SHAM), an inhibitor of the alternative oxidase pathway, affects the respiration rate of wild type and mutant plants differently, as it decreases the respiration rate of wild type leaves only about 8% but alters the respiration rate of the *cys-c1* mutant leaves by about 24% (Fig. 6B). In both wild type and mutant plants, the addition of KCN reduces the oxygen uptake drastically

to about 30% of the maximum respiration rate. The addition of KCN plus SHAM reduces oxygen uptake to levels lower than 10% (Fig. 6B). The increase of the alternative oxidase pathway in the *cys-c1* mutant correlates with an increase in transcript abundance of the *AOX1a* gene (Fig. 6C), which is induced by an alteration of the cytochrome respiration pathway (Albury et al., 2009; Garcia et al., 2010). In addition, the expression of *PR1*, a pathogenesis-related protein induced by the salicylic acid-dependent pathway (An and Mou, 2011), is induced in *cys-c1* plants in the absence of stress (Fig. 6C), suggesting that endogenously produced cyanide can modulate this pathway in Arabidopsis plants.

The *cys-c1* Mutant Accumulates Reactive Oxygen Species but Does not Show Programmed Cell Death Lesions

One of the earliest responses to pathogen infection is the production of reactive oxygen species (Lamb and Dixon, 1997), which together with nitric oxide (NO) and salicylic acid (SA), can promote the hypersensitive response (HR) (Delledonne et al., 1998; Alvarez, 2000) and lead to the activation of systemic acquired resistance (SAR), a broad spectrum form of disease resistance (Vlot et al., 2008). Since a reduction of the respiration rate can produce an accumulation of ROS, we compared the accumulation of ROS in *cys-c1* and wild type seedlings grown under control conditions (Fig. 7). Imaging of ROS *in vivo* in plant tissues by confocal laser microscopy is a very useful technique (Schneider et al., 1998). We observed a fluorescence emission resulting from the oxidation of the non-fluorescent dichlorofluorescein (H_2DCFDA) to a highly fluorescent product; this signal reflects significant production of H_2O_2. In roots, this fluorescence was higher in *cys-c1* specimens than in wild type samples (Fig. 7A-B). Although chlorophyll autofluorescence interferes with the H_2O_2 detection in green tissues, we were able to observe a higher fluorescence in *cys-c1* than in wild type cotyledons (Fig. 7C-D).

Because H_2O_2 is a signaling intermediate molecule in programmed cell death, we stained the leaves of plants grown in long-day and short-day conditions with lactophenol trypan blue. We did not observe lesions characteristic of spontaneous cell death in the leaves of the *cys-c1* mutant (Fig. 7E-H).

DISCUSSION

Plants synthesize ethylene in response to different environmental stimuli, including pathogen attack (Wang et al., 2002; Pandey and Somssich, 2009). The role of ethylene in defense signaling in plants has been studied extensively, but its involvement remains controversial. Treatment with ethylene increases or decreases resistance to pathogens depending on the plant-pathogen interaction, and the use of mutants defective in ethylene signaling indicates a limited or different role of ethylene in the resistance to some biotrophic and necrotrophic pathogens, including fungi, bacteria and virus (Pieterse et al., 1998; Brading et al., 2000; Broekaert et al., 2006; Iwai et al., 2006). Cyanide is produced concomitantly with ethylene biosynthesis. In this work, however, we show different patterns of ethylene and cyanide accumulation during infection of Arabidopsis with both the fungus *B. cinerea* and the virulent and avirulent *P. syringae.* In addition*,* we show that the lack of mitochondrial ß-cyanoalanine synthase of Arabidopsis, that leads to an accumulation of cyanide in plant tissues (García et al, 2010), results in an altered response to plant pathogens. The response is completely dependent on cyanide, as demonstrated by genetic and chemical complementation. All these data suggest that cyanide also acts in the regulation of the plant immune responses. Furthermore, the transcriptional regulation of the *CYS-C1* gene during the three plant-pathogen interactions analyzed allows a differential accumulation of cyanide in each interaction, suggesting that *CYS-C1* is involved in the signaling pathway, leading to resistance or sensitivity depending on the type of pathogen.

The classification of genes differentially expressed in *cys-c1* and wild type plants reveals that the high endogenous cyanide content of the *cys-c1* mutant is correlated with the biotic stress response. More specifically, the cyanide accumulation is correlated with the induction of genes encoding proteins involved in the plant signaling pathway. Among the induced genes in *cys-c1* mutant, three WRKY transcription factors, *WRKY18*, *33* and *40*, are involved in the modulation of host defenses toward phytopathogens (Pandey and Somssich, 2009). *WRKY33* in particular was shown to be required for resistance to the necrotrophs *A. brassicicola* and *B. cinerea* (Zheng et al., 2006), while WRKY18 and WRKY40 appear to be necessary for the resistance to *P. syringae* (Xu et al., 2006). Often, WRKY factors interact both physically and functionally in a complex pattern of overlapping or antagonistic roles. For instance, the

mutation of either *WRKY18* or *WRKY40* does not affect the susceptibility of plants to either necrotrophic or biotrophic pathogens. Double *WRKY18 WRKY40* mutants, however, are more susceptible to *P. syringae* and more resistant to *B. cinerea* than wild type plants (Xu et al., 2006). The simultaneous activation of *WRKY18*, *WRKY33* and *WRKY40* in the *cys-c1* mutant, then, does not necessarily lead to an additive effect for the expression of each WRKY factor separately. In fact, we have found that cyanide accumulation correlates with an increased susceptibility to a necrotrophic pathogen, and this association would probably be due to a deleterious but non-lethal effect of cyanide itself. An intriguing increase of the tolerance to biotrophic pathogens is observed concurrently. This increased tolerance is applicable to both a bacteria and a virus and occurs together with the induction of the pathogenesis-related *PR1* mRNA in the absence of pathogens. Both susceptibility to the necrotrophic fungus and resistance to the biotrophic bacteria are reversed by treatment with the antidote hydroxocobalamin, demonstrating that the effect observed is specifically related to cyanide. Although reactive oxygen species are more abundant in the *cys-c1* mutant than in wild type plants, no PCD lesions or microlesions are observed in the mutant, which demonstrates that cyanide does not induce a lesion-mimic phenotype that could be responsible for the resistance to *PstDC3000* (Lorrain et al., 2003)

To discriminate between distinctive pathogens and to activate appropriate responses, plants use phytohormones for signaling. In general, responses against biotrophic pathogens include a signaling cascade dependent on salicylic acid, while necrotrophic organisms induce signaling pathways dependent on ethylene and jasmonic acid (Pieterse et al., 2009). Interactions between the different signaling pathways have been demonstrated, indicating a complex network of hormone crosstalk (Koornneef and Pieterse, 2008; Spoel and Dong, 2008; Leon-Reyes et al., 2010). Exogenously applied cyanide mimics SA-induced resistance of tobacco, Arabidopsis and tomato plants to viruses (Chivasa and Carr, 1998; Wong et al., 2002). More recently, this treatment has been shown to confer resistance of rice to the biotrophic fungus *Magnaporthe oryzae* and it has been suggested that cyanide increases during the HR response (Seo et al., 2011). We have demonstrated that Arabidopsis plants accumulate more cyanide when they are infected with an avirulent strain of *Pst DC3000* than when they are challenged with the virulent strain, suggesting that this molecule has a role in the establishment of the hypersensitive response. The repression of *CYS-C1* expression during the avirulent interaction

and its activation during the virulent interaction further support this hypothesis. Finally, the resistance of the *cys-c1* mutant to biotrophic pathogens indicates that cyanide mimics or induces the SA signaling pathway in Arabidopsis plants.

Interestingly, *cys-c1* mutant leaves exhibit a reduced respiration rate that is more sensitive to the alternative pathway inhibitor SHAM and an enhanced expression of the *AOX1a* gene, showing that the alternative respiration pathway is activated in the mutant plants. AOX allows flexibility of plant respiratory metabolism, especially under environmental stresses (Vanlerberghe and McIntosh, 1997; Mackenzie and McIntosh, 1999), and it is induced by many adverse conditions (Hanqing et al., 2010). The induction of *AOX1a* in the *cys-c1* mutant in non-stressed conditions could prepare it to better respond to a pathogen attack, probably by inducing a signal transduction dependent on ROS that culminates in the induction of defense proteins such as PR1 and other proteins related to pathogenesis. It has been suggested that tobacco and tomato cyanide-induced resistance to virus is mediated by AOX, which would contribute to the signal transduction pathway leading to resistance (Chivasa and Carr, 1998; Fu et al., 2010). Strikingly, when over-expressing either the native AOX or a version of AOX mutated at its active site, TMV vectors increase systemic movements in *Nicotiana benthamiana* (Murphy et al., 2004).

In summary, our results suggest that cyanide, a low molecular weight and highly hydrophilic molecule, acts as a signal in plants. Nitric oxide and oxygen peroxide are also low molecular weight molecules that are toxic at high concentration but that exhibit a signaling role at low concentrations; their roles have been extensively demonstrated and accepted (Delledonne et al., 1998; Laloi et al., 2004). In our model, cyanide that is produced in the *cys-c1* mutant uncouples the respiratory electron chain dependent on the cytochrome c oxidase, and this uncoupling induces the alternative oxidase activity and the accumulation of reactive oxygen species which act by stimulating the salicylic acid-dependent signaling pathway of the plant immune system.

MATERIALS AND METHODS

Plant Material and Growth Conditions

Arabidopsis (*Arabidopsis thaliana*) wild type ecotype Col-0 and the SALK_022479 mutant were used in this work. The plants were grown in soil with a photoperiod of 8 h of white light (120 μE m^{-2} s^{-1}) at 20ºC/16 h of dark at 18ºC. Plants were cultivated for 6 to 7 weeks. For some experiments, the plants were cultivated in solid Murashige & Skoog media in Petri dishes supplemented with 1% sucrose with a photoperiod of 16 h of white light (120 μE m^{-2} s^{-1}) at 20ºC/8 h of dark at 18ºC.

To generate the *cys-c1* complementation line (*cys-c1*::Pcys-c1-*CYS-C1*), a 2949-bp genomic fragment containing the full-length coding sequence of *CYS-C1* plus the intergenic region between *CYS-C1* and its contiguous *PIP1* gene (At3g61430) was obtained by PCR amplification using the proofreading Platinum Pfx DNA polymerase (Invitrogen) and the primers C1GW-F and C1GW-R (Supplemental Table 3). The fragment was cloned into the pENTR/D-TOPO vector (Invitrogen) and transferred into the pMDC99 vector (Curtis and Grossniklaus, 2003) using the Gateway system (Invitrogen) according to the manufacturer's instructions. The final construct Pcys-c1-*CYS-C1* was generated by transformation into *Agrobacterium tumefaciens* and then introduced into *cys-c1* null plants using the floral-dip method (Clough and Bent, 1998).

Respiration measurements in leaves

Wild type and mutant plants were grown for 6 to 7 weeks in soil. Approximately 50 mg of leaf tissues was cut and transferred into air-tight cuvettes containing 20 mM Hepes (pH 7.2) and $CaCl_2$, and oxygen uptake was measured as a decrease of O_2 concentration in the dark using a Clark-type electrode. Cyanide-resistant O_2 uptake was measured in the presence of 0.5 mM KCN. The component of the change due to the alternative oxidase pathway was determined by measurement in the presence of 4 mM of the inhibitor SHAM.

Bacterial Pathogen Infections

The bacterial strains used in this study were *P. syringae pv. tomato* (*Pst*) *DC3000* and *Pst DC3000* bearing a plasmid containing the *avrRpm1* avirulence gene (Grant et al., 1995). For the treatment of the plants, bacterial cultures were collected from plates in 10 mM $MgCl_2$ and

their concentrations were adjusted to $5x10^6$ bacteria ml^{-1} (DO_{600}=0.01, *Pst DC3000 avrRpm1*) or $2.5x10^6$ bacteria ml^{-1} (DO_{600}=0.005, *Pst DC3000*). Sterile 10 mM $MgCl_2$ was used as a mock solution. The bacterial suspension or the mock solution was then pressure infiltrated into the abaxial side of the leaves of 6- to 7-week-old plants using a syringe without a needle. Wild type,, mutant and complemented plants were grown at the same time using the same conditions (Swanson *et al*., 1988).

Bacteria and Growth Tests

Pst DC3000 avrRpm1 bacteria were collected from LB plates supplemented with rifampicine (50 µg ml^{-1}) in 10 mM $MgCl_2$ and their concentration was adjusted to $5x10^6$ bacteria ml^{-1} (DO_{600}=0.01). To determine whether hydroxocobalamin affects bacterial viability, growth tests were performed as described previously (Alvarez et al., 2012a) by supplementing the growth medium with hydroxocobalamin 5 mM instead of cysteine 0.5 mM. Six series of 1:10 dilutions were performed. In all, 10 µl of the resulting suspensions was plated, grown for 48 h at 28ºC and subsequently photographed (Supplemental Fig. S13).

In Planta* Growth of Virulent or Avirulent *Pseudomonas syringae DC3000

The protocol for measuring the growth of bacteria was adapted from (Tornero and Dangl, 2001). Wild type, mutant and complemented plants were grown for 6 to 7 weeks at the same time and in the same conditions and inoculated with bacterial pathogens as described above. One hour after the inoculation, the samples for Day 0 were taken. To determine bacterial growth, 100 mg of leaves was ground in 500 µl of 10 mM $MgCl_2$ and gently vortexed. In all, 20 µl from each sample was added to the wells of a microtiter plate containing 180 µl of 10 mM $MgCl_2$ and serial 10-fold dilutions were plated on Petri dishes containing 50 mg mL^{-1} rifampicin. The plates were incubated at 30°C and the number of colonies was counted 30 h later. The number of colony forming units (cfu) mg^{-1} fresh weight was determined by the formula cfu mg^{-1} FW = k (N x $10^{d\ -1}$)/(weight of the tissue), where N is the number of colonies counted in the dilution number d and the constant k (500 in our case) represents the

number of cfu present in the sample per colony appearing in the first dilution (Tornero and Dangl, 2001).

Fungal Infections

The *Botrytis cinerea* strain ME4 was grown in a solid strawberry broth for 12 days, and spore suspensions were prepared at a concentration of $5x10^5$ spores mL^{-1} in 12 g L^{-1} Potato-Dextrose-Broth (PDB). Six- to seven-week-old wild type, mutant and complemented plants grown at the same time and in the same conditions were pulverized with a Preval sprayer with spore suspension. Approximately 2 mL of spore suspension per plant was used. The plants were covered with a transparent film to maintain 100% humidity. The samples were collected for PCR analysis after five days.

Quantification of *B. cinerea* DNA Accumulation in Infected Plants

DNA from infected plants was quantified by real-time PCR according to a previous study (Calo et al., 2006). DNA from the *B. cinerea creA* gene (Tudzynski et al., 2000) was amplified using the oligonucleotides *creABOT-F* and *creABOT-R* (Supplemental Table S3). As an internal standard to normalize the qPCR, *A. thaliana UBQ10* DNA was amplified using the oligonucleotides *UBQ10F* and *UBQ10R* (Supplemental Table S3). Relative quantifications were performed by subtracting the cycle threshold (CT) value of *UBQ10* from the CT value of *creA* (ΔCT). The percentage of *B. cinerea* DNA was calculated as $(2^{-\Delta CT\ mutant} * 100)/ 2^{-\Delta CT\ wild\ type}$.

Geminivirus Infections Assays

BCTV (*Beet curly top virus*) infections of Arabidopsis plants were performed by whole plant agroinoculation as described in (Briddon et al., 1989; Lozano-Duran et al., 2011). Inoculated plants were scored for the appearance of symptoms typical of a BCTV infection on systemically infected tissue. Symptom severity was evaluated at 28 days post infection (dpi) according to the severity index described in (Baliji et al., 2007), where 0 represents

symptomless plants and 1 to 4 represent plants showing increasing symptom severity. The infection assay was performed in triplicate.

Quantification of BCTV DNA Accumulation in Infected Plants

Total DNA of infected plants was extracted at 28 dpi using the DNeasy Plant Mini Kit (Qiagen) and digested with DpnI to differentiate between viral DNA originating from a replication *in planta*, which is not methylated, and viral DNA originating from replication in the inoculum of *A. tumefaciens*, which is methylated. Viral DNA accumulation was quantified by qPCR using the primers BCTV-F and BCTV-R (Supplemental Table S2). As an internal standard to normalize the qPCR, *A. thaliana UBQ10* DNA was amplified using the oligonucleotides qUBQ10F and qUBQ10R (Supplemental Table S3). Relative quantifications were performed by subtracting the cycle threshold (CT) value of *UBQ10* from the CT value of *BCTV* (ΔCT). The relative BCTV DNA was calculated as $2^{-\Delta CT}$.

H_2O_2 Detection

For the fluorimetric detection of H_2O_2, five-day-old seedlings were incubated with 10 µM H_2DCFDA (2',7'-dichlorodihydrofluorescein diacetate, Molecular Probes, Eugene, OR, USA) for 5 min in the presence of 10 µM propidium iodide (Lopez-Martin et al., 2008). Samples were observed using a Leica TCS SP2 spectral confocal microscope with an excitation of 488 nm and an emission range of 500-550 nm for fluorescein detection and 600-650 nm for propidium iodide detection.

Cell Death Staining

Trypan blue staining for dead cells in leaves was performed as described previously (Carol and Dolan, 2006) by incubating the leaves in a lactic acid-phenol-trypan blue solution (2.5 mg/mL trypan blue, 25% [w/v] lactic acid, 23% phenol, 25% glycerol), heating them over boiling water for 1 min and finally destaining them using a 2.5 g/mL chloral hydrate solution before photographing the leaves.

Ethylene Determination by Gas Chromatography

A total of 100-300 mg of infected leaves was collected, weighted, placed inside a 12 ml vial and finally sealed. The amount of ethylene produced and released to the gas phase during 24h was determined by gas chromatography by injecting 1 ml of the head space onto a GC2010 equipped with an activated alumina column and a FID. The oven and the detector temperatures were isothermally maintained at 80 and 150 °C, respectively. The results were expressed as the mean ± SD from at least five replica samples, and the experiment was repeated three times from independent samples.

Cyanide Determination by HPLC

100 mg of plant tissue was homogenized using a mortar and pestle with liquid nitrogen and resuspended in cold borate-phosphate extraction buffer (2 ml per g of fresh weight) containing 27 mM sodium borate and 47 mM potassium phosphate, pH 8.0. Homogenates were centrifuged at 15,000 g for 15 min at 4ºC. Extracted cyanide was subsequently quantified by reverse-phase HPLC after derivatization with 2,3-naphthalenedialdehyde (NDA) to form a 1-cyano-2-alkyl-benz[f]isoindole (CBI) derivative by previously described methods (Lin et al., 2005; Garcia et al., 2010).

RNA Isolation and Semiquantitative RT-PCR Reaction

Total RNA was extracted from Arabidopsis leaves using the RNeasy Plant Mini Kit (Qiagen) and reverse transcribed using an oligo(dT) primer and the SuperScript First-Strand Synthesis System for RT-PCR (Invitrogen) following the manufacturer's instructions. *AOX1a* and *PR1* expression was determined by semiquantitative PCR using an aliquot of the cDNA and the oligonucleotides shown in Supplemental Table S3. The constitutively expressed *UBQ10* gene was used as a control. The PCR conditions were as follows: a denaturation cycle of 2 min at 94º C; 30 amplification cycles of 1 min at 94º C, 1 min at 60º C and 1 min at 72º C; and an extension cycle of 5 min at 72º C.

Real-Time RT-PCR

Quantitative real-time RT-PCR was used to validate microarray data and to analyze the expression of the *CYS-C1* gene. First-strand cDNA was synthesized as described above. Gene-specific primers for each gene were designed using the Vector NTI Advance 10 software (Invitrogen; Supplemental Table S3). Real-time PCR was performed using iQ SYBR Green Supermix (Bio-Rad) and the signals were detected on an iCYCLER (Bio-Rad) according to the manufacturer's instructions. The cycling profile consisted of 95ºC for 10 min followed by 45 cycles of 95ºC for 15 s and 60ºC for 1 min. A melt curve from 60ºC to 90ºC was run following the PCR cycling. The expression levels of each gene were normalized to those of the constitutive *UBQ10* gene by subtracting the cycle threshold (CT) value of *UBQ10* from the CT value of the gene (ΔCT). The fold change was calculated as $2^{-(\Delta CT \text{ mutant} - \Delta CT \text{ wild type})}$.

RNA Extraction and Microarray Hybridization

For microarray studies of the *cys-c1* mutant, plants were grown in MS plates supplemented with 1% sucrose under a photoperiod of 16 h of white light (120 µE m^{-2} s^{-1}) at 20ºC/8 h of dark at 18ºC. Leaves of 15-day-old plants were used for total RNA isolation with TRIzol reagent (Invitrogen) and cleaning with the RNeasy Plant Mini Kit (Qiagen). The resulting material was used to synthesize biotinylated cRNA for hybridization to Arabidopsis ATH1 arrays (Affymetrix, Santa Clara, CA) using the 3´ Amplification One-Cycle Target Labeling Kit. Briefly, 4 mg of RNA was reverse transcribed to produce first strand cDNA using a $(dT)_{24}$ primer with a T7 RNA polymerase promoter site added to the 3' end. After second strand synthesis, *in vitro* transcription was performed using T7 RNA polymerase and biotinylated nucleotides to produce biotin-labeled cRNA. The cRNA preparations (15 µg) were fragmented into fragments of 35 to 200 bp at 95°C for 35 min. These fragmented cRNAs were hybridized to the Arabidopsis ATH1 microarrays at 45°C for 16 h. Each microarray was washed and stained in the Affymetrix Fluidics Station 400 following standard protocols. Microarrays were scanned using an Affymetrix GeneChip® Scanner 3000.

Microarray Data Analysis

Microarray analysis was performed using the affylmGUI R package (Wettenhall et al., 2006). The Robust Multi-array Analysis (RMA) algorithm was used for background correction, normalization and summarizing expression levels (Irizarry et al., 2003). Differential expression analysis was performed using Bayes t-statistics and the linear models for microarray data (Limma), which are included in the affylmGUI package. *p*-values were corrected for multiple testing using Benjamini-Hochberg's method (False Discovery Rate) (Benjamini and Hochberg, 1995; Reiner et al., 2003). Cutoff values of 2-fold change and *p*-value of less than 0.05 were adopted to discriminate expression of genes that were differentially expressed in the mutant plant with respect to the wild type. Gene classification into functional groups was determined using the Bio-Array Resource for Arabidopsis Functional Genomics (Toufighi et al., 2005) and MapMan software (http://gabi.rzpd.de/projects/MapMan/). The microarray data for the *cys-c1* mutant were meta-analyzed using Genevestigator (Hruz et al., 2008).

Statistical Analysis

For all the experiments shown, at least three independent samples were analyzed (for details, see the legend of the respective figures). An ANOVA statistical analysis of data was performed using the program OriginPro 7.5 (OriginLab Corporation).

Acknowledgments

We would like to acknowledge Dr. Olga Del Pozo for providing the bacterial strains used in this work.

Figure legends

Figure 1. Time-course of the accumulation of ethylene (A) and cyanide (B) and the regulation of *CYS-C1* transcript (C) during the *A. thaliana-B. cinerea* interaction. Ethylene (A) and cyanide (B) were measured in leaf extracts of wild type plants grown for 6 to 7 weeks and infected with a spore suspension of *B. cinerea*. The results presented here are expressed as the mean ± standard deviation (SD) of a representative experiment in which 12-14 leaves from infected plants were pooled and three independent extractions were made from the pooled material. The experiment was repeated three times, with similar results obtained each time. The expression level of *CYS-C1* (C) was analyzed by real-time RT-PCR and referred to the *UBQ10* internal control. The data correspond to the means ± SD of three independent analyses using material grown in different batches at different times. For each analysis, 5-6 plants were pooled, and three independent RNA extractions were made from the pooled material. Two experimental replicates were made for each sample. The data were normalized against the data obtained from plants treated with a mock solution. hpi, hours post-infection. Not-normalized data are shown in Supplemental Fig. S7A, S8A and S9A.

Figure 2. Time-course of the accumulation of ethylene (A) and cyanide (B) and the regulation of *CYS-C1* transcript (C) during the *A. thaliana-P. syringae* interactions. Ethylene (A) and cyanide (B) were measured in leaf extracts of wild type plants grown for 6 to 7 weeks and infected with a bacterial suspension of either *Pst DC3000* or *Pst DC3000 avrRpm1* as described in the Material and Methods. The results presented here are expressed as the mean ± SD of a representative experiment in which 12-14 leaves from infected plants were pooled and three independent extractions were made from the pooled material. The experiment was repeated three times, with similar results obtained each time. The expression level of *CYS-C1* (C) was analyzed by real-time RT-PCR and referred to the *UBQ10* internal control. The data correspond to the means ± SD of three independent analysis using material grown in different batches at different times. For each analysis, 5-6 plants were pooled, and three independent RNA extractions were made from the pooled material. Moreover, two experimental replicates were made for each sample. The data were normalized against the data obtained from plants

treated with a mock solution. hpi, hours post-infection. Not-normalized data are shown in Supplemental Fig. S7B, S8B and S9B.

Figure 3. Responses of the *cys-c1* mutant to pathogen infection. A, B, Susceptibility of wild type and *cys-c1* mutant to *Botrytis cinerea* infection. A. Wild type and *cys-c1* mutant plants after 5 days of *B. cinerea* infection. B. Quantification of fungus growth was performed by real-time-PCR amplification of the *B. cinerea creA* gene, which was normalized against the Arabidopsis *UBQ10* gene. DNA was isolated from leaves 5 days after spore inoculation of 6- to 7-week-old wild type and mutant plants grown in parallel. The data correspond to the mean ± standard deviation (SD) of at least three independent analysis made from material grown in different batches at different times. For each analysis, twenty infected plants were pooled, and six independent DNA extractions were made from the pooled material. Moreover, two experimental replicates were made from each sample. C, D, Susceptibility of wild type and *cys-c1* mutants to infection with virulent *Pst DC3000* bacteria. C. Wild type and *cys-c1* mutant leaves after 3 days of *Pst DC3000* infection. *cys-c1* leaves show less severe symptoms than wild type. D. Colony-forming units (cfu) were counted at 0, 2 and 4 days post-infection (dpi) of 6- to 7-week-old wild type and mutant plants grown in parallel. At total of 12 to 14 leaves were pooled for each analysis, in which three independent counts were made from the pooled material and two experimental replicates were made from each sample. The data correspond to the mean ± standard deviation (SD) of one representative experiment. *, $P<0.05$. The experiment was performed three times with material grown in different batches at different times; similar results were obtained for each iteration.

Figure 4. Hydroxocobalamin effect on plant susceptibility to pathogens. Wild type and *cys-c1* mutant plants were infected with *B. cinerea* (A) or *Pst DC3000* (B), as indicated in the Material and Methods. Pathogens were collected in suspensions containing (+COB) or not containing (-COB) hydroxocobalamin at the concentration indicated and used to perform the susceptibility assays. Quantification of fungus growth was performed by real-time-PCR amplification of the *B. cinerea creA* gene, which was normalized against the Arabidopsis *UBQ10* gene. DNA was isolated from leaves 5 days after spore inoculation of 6- to 7-week-old wild type and mutant plants grown in parallel. Colony-forming units (cfu) were counted at

3 days post-infection, with 12 to 14 leaves pooled for each analysis. Three independent determinations were made from the pooled material, and two experimental replicates were made from each sample. The data correspond to the mean ± standard deviation (SD) of one representative experiment. *, $P<0.05$

Figure 5. Response of the *cys-c1* mutant to virus. A, Example of the severity index described in Materials and Methods and Baliji *et al.* (2007). 0: no symptoms; 1 to 4, increasing severity of symptoms. B, Susceptibility of wild type and *cys-c1* mutant to BCTV infection. Whole six- to seven-week-old plants of each genotype were agroinoculated, and the symptom severity was recorded at 28 dpi. C, Quantification of virus growth was performed in the same plants at 28 dpi by real-time PCR amplification of the viral DNA, which was normalized against the Arabidopsis *UBQ10* gene. The data correspond to the mean ± standard deviation (SD) of three independent analyses made from material grown in different batches at different times. For each analysis, at least ten infected plants were pooled, and six independent DNA extractions were made from the pooled material. Two experimental replicates were performed from each sample. *, $P<0.05$

Figure 6. Respiration rates (A, B) and *AOX1a* and *PR1* expression levels (C) in leaves of wild type and *cys-c1* mutant plants. Cyanide-independent and alternative oxidase respiration were determined in the presence of 0.5 mM KCN or 4 mM SHAM, respectively. The transcription level of the alternative oxidase gene *AOX1a, PR1* and the control *UBQ10* was determined by RT-PCR in leaves of non infected 6- to 7-week-old plants. The data correspond to the mean ± standard deviation (SD) of at least three independent analysis made from material grown in different batches at different times. *, $P<0.05$.

Figure 7. Accumulation of H_2O_2 and lesion formation in wild type and *cys-c1* mutant. H_2O_2 was detected by H_2DCFDA staining in root (A-B) and cotyledons (C-D) from five-days-old wild type and *cys-c1* mutant plants cultured in MS medium. Lactophenol trypan blue was used to stain spontaneous cell death lesions (E-H). Detached leaves of plants grown in soil for three weeks in long-day conditions (E-F) or 6-7 weeks in short-day conditions (G-H)

were used for the assay. All the experiments were repeated at least three times, with similar results obtained each time.

Supporting Data

Supplemental Figure S1. Analysis of the *cys-c1* transcriptome. Data were analyzed using the Classification SuperViewer tool of the Bio-Array Resource for Arabidopsis Functional Genomics, BAR (Toufighi et al., 2005). A functional classification of all the deregulated genes in the *cys-c1* mutant based on the GO database and a ranking score for each functional class are shown.

Supplemental Figure S2. Relative expression levels of selected genes in the *cys-c1* mutant plants. Real-time RT-PCR analysis of expression of the *WRKY33 (At2g38470), ERF6 (At4g17490), CYP81F2 (At5g57220)* and *GSTU24 (At1g17170)* genes was performed in 15-day-old seedlings. The transcript levels were normalized to the internal control, the constitutive *UBQ10* gene. Data shown are means $\pm$ SD of three independent analyses and represent the transcript level of each gene in the *cys-c1* mutant plants relative to the transcript level in the Col-0 plants.

Supplemental Figure S3. Graphic display of the hierarchical clustering of *cys-c1* up- or down-regulated genes in response to hypoxia, performed with Genevestigator (Hruz et al., 2008). Each row represents the treatment indicated, and each column refers to a gene. A dendrogram representing the Euclidian distance between mutants is shown, and the scale to the top marks the correlation coefficient represented by the length of the branches that connect pairs of nodes. The color scale indicates the $\log_2$ level of expression above (red) or below (green) the median.

Supplemental Figure S4. Graphic display of meta-profile analysis of *cys-c1* up- or down-regulated genes in response to biotic stresses, performed with Genevestigator (Hruz et al., 2008). See the legend of figure S3 for details.

Supplemental Figure S5. Graphic display of hierarchical clustering of *cys-c1* up- or down-regulated genes in response to elicitors and pathogens, performed with Genevestigator (Hruz et al., 2008). See the legend of figure S3 for details.

Supplemental Figure S6. Graphic display of hierarchical clustering of *cys-c1* up- or down-regulated genes in response to ACC treatment and in the *etr1-1* mutant, performed with Genevestigator (Hruz et al., 2008). See the legend of figure S3 for details

Supplemental Figure S7. Time-course of the accumulation of ethylene during the *A. thaliana-B. cinerea* interaction (A) and the *A. thaliana-P. syringae* interacions (B). Ethylene was measured in leaf extracts of wild type plants grown for 6 to 7 weeks and mock-treated or infected with a spore suspensions of *B. cinerea* (BOT) or a bacterial suspension of either *Pst DC3000* or *Pst DC3000 avrRpm1* as described in Material and Methods. The results presented here are expressed as the mean ± SD of a representative experiment in which 10-12 independent measurements were done. The experiment was repeated three times, with similar results obtained each time. hpi, hours post-infection

Supplemental Figure S8. Time-course of the accumulation of cyanide during the *A. thaliana-B. cinerea* interaction (A) and the *A. thaliana-P. syringae* interacions (B). Cyanide was measured in leaf extracts of wild type plants grown for 6 to 7 weeks and mock-treated or infected with a spore suspensions of *B. cinerea* (BOT) or a bacterial suspension of either *Pst DC3000* or *Pst DC3000 avrRpm1* as described in Material and Methods. The results presented here are expressed as the mean ± SD of a representative experiment in which 12-14 leaves from infected plants were pooled and three independent extractions were made from the pooled material. The experiment was repeated three times, with similar results obtained each time. hpi, hours post-infection.

Supplemental Figure S9. Time-course of the expression of *CYS-C1*during the *A. thaliana-B. cinerea* interaction (A) and the *A. thaliana-P. syringae* interacions (B). *CYS-C1* expression was measured in leaf extracts of wild type plants grown for 6 to 7 weeks and mock-treated or infected with a spore suspensions of *B. cinerea* (BOT) or a bacterial suspension of either *Pst*

DC3000 or *Pst DC3000 avrRpm1* as described in Material and Methods. The expression level of *CYS-C1* was analyzed by real-time RT-PCR and referred to the *UBQ10* internal control. The data correspond to the means ± SD of three independent analysis using material grown in different batches at different times. For each analysis, 5-6 plants were pooled, and three independent RNA extractions were made from the pooled material. Moreover, two experimental replicates were made for each sample. hpi, hours post-infection.

Supplemental Figure S10. Susceptibility of wild type and *cys-c1* mutant to infection with avirulent *Pst DC3000 avrRpm1* bacteria. Colony-forming units (cfu) were counted at 0, 1 and 3 days post-infection of 6- to 7-week-old wild type and mutant plants grown in parallel. At total of 12 to 14 leaves were pooled for each analysis, in which three independent counts were made from the pooled material and two experimental replicates were made from each sample. The data correspond to the mean ± standard deviation (SD) of one representative experiment. The experiment was performed three times with material grown in different batches at different times; similar results were obtained for each iteration.

Supplemental Figure S11. Genetic complementation of the pathogen-associated phenotype of the *cys-c1* mutant. Wild type, *cys-c1* mutant and complemented *cys-c1*::Pcys-c1-*CYS-C1* plants were infected with *B. cinerea* (A) and the virulent *Pst DC3000* (B, C) as indicated in Figure 3. (A) Quantification of fungus growth was performed by real-time-PCR amplification of the *B. cinerea creA* gene, which was normalized against the Arabidopsis *UBQ10* gene. DNA was isolated from leaves 5 days after spore inoculation of 6- to 7-week-old wild type, mutant and complemented plants grown in parallel. (B) Wild type, *cys-c1* mutant and the complemented *cys-c1*::Pcys-c1-*CYS-C1* plant leaves after 3 days of *Pst DC3000* infection. (C) Colony-forming units (cfu) were counted at 3 days post-infection (dpi). A total of 12 to 14 leaves were pooled for each analysis. Three independent determinations were made from the pooled material, and two experimental replicates were made from each sample. The data correspond to the mean ± standard deviation (SD) of one representative experiment. *, $P<0.05$

Supplemental Figure S12. Dose-dependent effect of the hydroxocobalamin on plant susceptibility to *B. cinerea*. Wild type and *cys-c1* mutant plants were infected with *B. cinerea* as indicated in Figure 4. Pathogens were collected in suspensions containing (+COB) or not containing (-COB) hydroxocobalamin at 5 mM and were used to perform the susceptibility assays. A total of 12 to 14 leaves were pooled for each analysis, in which three independent determinations were made from the pooled material and two experimental replicates were made from each sample. The data correspond to the mean ± standard deviation (SD) of one representative experiment. *, $P<0.05$

Supplemental Figure S13. Growth tests of *Pst DC3000* bacteria grown in LB medium supplemented with rifampicine and hydroxocobalamin 5 mM (COB 5 mM) or with rifampicine alone (-COB). a to d: 10 µl of serial 10-fold dilutions of a $5x10^6$ bacteria ml^{-1} *Pst DC3000* suspension.

Supplemental Table S1. List of differentially regulated genes in leaves of the cys-c1 mutant compared to wild type

Supplemental Table S2. Pathogen and hypoxia-regulated genes in the *cys-c1* mutant.

Supplemental Table S3. Oligonucleotide sequences used in this work.

LITERATURE CITED

AbuQamar, S., Chen, X., Dhawan, R., Bluhm, B., Salmeron, J., Lam, S., Dietrich, R.A., Mengiste, T. (2006). Expression profiling and mutant analysis reveals complex regulatory networks involved in Arabidopsis response to Botrytis infection. Plant J **48:** 28-44.

Albury, M.S., Elliott, C., Moore, A.L. (2009). Towards a structural elucidation of the alternative oxidase in plants. Physiol Plant **137:** 316-327.

Alvarez, C., Calo, L., Romero, L.C., Garcia, I., Gotor, C. (2010). An O-acetylserine(thiol)lyase homolog with L-cysteine desulfhydrase activity regulates cysteine homeostasis in Arabidopsis. Plant Physiol **152:** 656-669.

Alvarez, C., Bermudez, M.A., Romero, L.C., Gotor, C., Garcia, I. (2012a). Cysteine homeostasis plays an essential role in plant immunity. New Phytol **193:** 165-177.

Álvarez, C., García, I., Romero, L.C., Gotor, C. (2012b). Mitochondrial Sulfide Detoxification Requires a Functional Isoform O-Acetylserine(thiol)lyase C in Arabidopsis thaliana. Mol Plant **5:** 1217-1226.

Alvarez, M.E. (2000). Salicylic acid in the machinery of hypersensitive cell death and disease resistance. Plant Mol Biol **44:** 429-442.

An, C., Mou, Z. (2011). Salicylic Acid and its Function in Plant ImmunityF. Journal of Integrative Plant Biology **53:** 412-428.

Astier, A., Baud, F.J. (1996). Complexation of intracellular cyanide by hydroxocobalamin using a human cellular model. Hum Exp Toxicol **15:** 19-25.

Baliji, S., Sunter, J., Sunter, G. (2007). Transcriptional analysis of complementary sense genes in Spinach curly top virus and functional role of C2 in pathogenesis. Mol Plant Microbe Interact **20:** 194-206.

Benjamini, Y., Hochberg, Y. (1995). Controlling the False Discovery Rate - a Practical and Powerful Approach to Multiple Testing. Journal of the Royal Statistical Society Series B-Methodological **57:** 289-300.

Bent, A.F., Kunkel, B.N., Dahlbeck, D., Brown, K.L., Schmidt, R., Giraudat, J., Leung, J., Staskawicz, B.J. (1994). RPS2 of Arabidopsis thaliana: a leucine-rich repeat class of plant disease resistance genes. Science **265:** 1856-1860.

Bermudez, M.A., Paez-Ochoa, M.A., Gotor, C., Romero, L.C. (2010). Arabidopsis S-sulfocysteine synthase activity is essential for chloroplast function and long-day light-dependent redox control. Plant Cell **22:** 403-416.

Bethke, P.C., Libourel, L.G.L., Reinohl, V., Jones, R.L. (2006). Sodium nitroprusside, cyanide, nitrite, and nitrate break Arabidopsis seed dormancy in a nitric oxide-dependent manner. Planta **223:** 805-812.

Bogatek, R., Dziewanowska, K., Lewak, S. (1991). HYDROGEN-CYANIDE AND EMBRYONAL DORMANCY IN APPLE SEEDS. Physiol Plant **83:** 417-421.

Borowitz, J.L., Gunasekar, P.G., Isom, G.E. (1997). Hydrogen cyanide generation by mu-opiate receptor activation: possible neuromodulatory role of endogenous cyanide. Brain Res **768:** 294-300.

Borron, S.W., Baud, F.J., Megarbane, B., Bismuth, C. (2007). Hydroxocobalamin for severe acute cyanide poisoning by ingestion or inhalation. Am J Emerg Med **25:** 551-558.

Bottcher, C., Westphal, L., Schmotz, C., Prade, E., Scheel, D., Glawischnig, E. (2009). The multifunctional enzyme CYP71B15 (PHYTOALEXIN DEFICIENT3) converts cysteine-indole-3-acetonitrile to camalexin in the indole-3-acetonitrile metabolic network of Arabidopsis thaliana. Plant Cell **21:** 1830-1845.

Brading, P.A., Hammond-Kosack, K.E., Parr, A., Jones, J.D. (2000). Salicylic acid is not required for Cf-2- and Cf-9-dependent resistance of tomato to Cladosporium fulvum. Plant J **23:** 305-318.

Briddon, R.W., Watts, J., Markham, P.G., Stanley, J. (1989). The coat protein of beet curly top virus is essential for infectivity. Virology **172:** 628-633.

Broekaert, W.F., Delaure, S.L., De Bolle, M.F., Cammue, B.P. (2006). The role of ethylene in host-pathogen interactions. Annu Rev Phytopathol **44:** 393-416.

Calo, L., Garcia, I., Gotor, C., Romero, L.C. (2006). Leaf hairs influence phytopathogenic fungus infection and confer an increased resistance when expressing a Trichoderma alpha-1,3-glucanase. J Exp Bot **57:** 3911-3920.

Carol, R.J., Dolan, L. (2006). The role of reactive oxygen species in cell growth: lessons from root hairs. J Exp Bot **57:** 1829-1834.

Chivasa, S., Carr, J.P. (1998). Cyanide restores N gene-mediated resistance to tobacco mosaic virus in transgenic tobacco expressing salicylic acid hydroxylase. Plant Cell **10:** 1489-1498.

Christianson, J.A., Wilson, I.W., Llewellyn, D.J., Dennis, E.S. (2009). The Low-Oxygen-Induced NAC Domain Transcription Factor ANAC102 Affects Viability of Arabidopsis Seeds following Low-Oxygen Treatment. Plant Physiol **149:** 1724-1738.

Cipollone, R., Visca, P. (2007). Is there evidence that cyanide can act as a neuromodulator? IUBMB Life **59:** 187-189.

Clough, S.J., Bent, A.F. (1998). Floral dip: a simplified method for Agrobacterium-mediated transformation of Arabidopsis thaliana. Plant J **16:** 735-743.

Cohn, M.A., Hughes, J.A. (1986). Seed dormancy in red rice. 5. Response to azide, hydroxylamine and cyanide. Plant Physiol **80:** 531-533.

Cristescu, S.M., De Martinis, D., Te Lintel Hekkert, S., Parker, D.H., Harren, F.J. (2002). Ethylene production by Botrytis cinerea in vitro and in tomatoes. Appl Environ Microbiol **68:** 5342-5350.

Curtis, M.D., Grossniklaus, U. (2003). A gateway cloning vector set for high-throughput functional analysis of genes in planta. Plant Physiol **133:** 462-469.

Delledonne, M., Xia, Y., Dixon, R.A., Lamb, C. (1998). Nitric oxide functions as a signal in plant disease resistance. Nature **394:** 585-588.

Donato, D.B., Nichols, O., Possingham, H., Moore, M., Ricci, P.F., Noller, B.N. (2007). A critical review of the effects of gold cyanide-bearing tailings solutions on wildlife. Environ Int **33:** 974-984.

Fol, M., Frachisse, J.M., Petel, G., Gendraud, M. (1989). Effect of cyanide on the membrane-potential of jerusalem artichoke (Helianthus-tuberosus l) tuber-parenchyma - Different responses in relation to dormancy. Comptes Rendus De L Academie Des Sciences Serie Iii-Sciences De La Vie-Life Sciences **309:** 551-556.

Fu, L.J., Shi, K., Gu, M., Zhou, Y.H., Dong, D.K., Liang, W.S., Song, F.M., Yu, J.Q. (2010). Systemic induction and role of mitochondrial alternative oxidase and nitric oxide in a compatible tomato-Tobacco mosaic virus interaction. Mol Plant Microbe Interact **23:** 39-48.

Garcia, I., Castellano, J.M., Vioque, B., Solano, R., Gotor, C., Romero, L.C. (2010). Mitochondrial beta-cyanoalanine synthase is essential for root hair formation in Arabidopsis thaliana. Plant Cell **22:** 3268-3279.

Glawischnig, E. (2007). Camalexin. Phytochemistry **68:** 401-406.

Glazebrook, J. (2005). Contrasting mechanisms of defense against biotrophic and necrotrophic pathogens. Annu Rev Phytopathol **43:** 205-227.

Grant, M.R., Godiard, L., Straube, E., Ashfield, T., Lewald, J., Sattler, A., Innes, R.W., Dangl, J.L. (1995). Structure of the Arabidopsis RPM1 gene enabling dual specificity disease resistance. Science **269:** 843-846.

Gunasekar, P.G., Borowitz, J.L., Turek, J.J., Van Horn, D.A., Isom, G.E. (2000). Endogenous generation of cyanide in neuronal tissue: Involvement of a peroxidase system. J Neurosci Res **61:** 570-575.

Gunasekar, P.G., Prabhakaran, K., Li, L., Zhang, L., Isom, G.E., Borowitz, J.L. (2004). Receptor mechanisms mediating cyanide generation in PC12 cells and rat brain. Neurosci Res **49:** 13-18.

Hall, A.H., Dart, R., Bogdan, G. (2007). Sodium thiosulfate or hydroxocobalamin for the empiric treatment of cyanide poisoning? Ann Emerg Med **49:** 806-813.

Han, L., Li, G.J., Yang, K.Y., Mao, G., Wang, R., Liu, Y., Zhang, S. (2010). Mitogen-activated protein kinase 3 and 6 regulate Botrytis cinerea-induced ethylene production in Arabidopsis. Plant J **64:** 114-127.

Hanqing, F., Kun, S., Mingquan, L., Hongyu, L., Xin, L., Yan, L., Yifeng, W. (2010). The expression, function and regulation of mitochondrial alternative oxidase under biotic stresses. Mol Plant Pathol **11:** 429-440.

Hartley, S.A., Kato, K., Salter, K.J., Kozlowski, R.Z. (1998). Functional evidence for a novel suramin-insensitive pyrimidine receptor in rat small pulmonary arteries. Circ Res **83:** 940-946.

Hruz, T., Laule, O., Szabo, G., Wessendorp, F., Bleuler, S., Oertle, L., Widmayer, P., Gruissem, W., Zimmermann, P. (2008). Genevestigator v3: a reference expression database for the meta-analysis of transcriptomes. Adv Bioinformatics **2008:** 420747.

Irizarry, R.A., Hobbs, B., Collin, F., Beazer-Barclay, Y.D., Antonellis, K.J., Scherf, U., Speed, T.P. (2003). Exploration, normalization, and summaries of high density oligonucleotide array probe level data. Biostatistics **4:** 249-264.

Isom, G.E., Way, J.L. (1984). Effects of oxygen on the antagonism of cyanide intoxication: cytochrome oxidase, in vitro. Toxicol Appl Pharmacol **74:** 57-62.

Iwai, T., Miyasaka, A., Seo, S., Ohashi, Y. (2006). Contribution of ethylene biosynthesis for resistance to blast fungus infection in young rice plants. Plant Physiol **142:** 1202-1215.

Jones, J.D., Dangl, J.L. (2006). The plant immune system. Nature **444:** 323-329.

Koornneef, A., Pieterse, C.M. (2008). Cross talk in defense signaling. Plant Physiol **146:** 839-844.

Laloi, C., Apel, K., Danon, A. (2004). Reactive oxygen signalling: the latest news. Curr Opin Plant Biol **7:** 323-328.

Lamb, C., Dixon, R.A. (1997). The Oxidative Burst in Plant Disease Resistance. Annu Rev Plant Physiol Plant Mol Biol **48:** 251-275.

Leon-Reyes, A., Van der Does, D., De Lange, E.S., Delker, C., Wasternack, C., Van Wees, S.C., Ritsema, T., Pieterse, C.M. (2010). Salicylate-mediated suppression of jasmonate-responsive gene expression in Arabidopsis is targeted downstream of the jasmonate biosynthesis pathway. Planta **232:** 1423-1432.

Lin, C.C., Wong, B.K., Burgey, C.S., Gibson, C.R., Singh, R. (2005). In vitro metabolism of a thrombin inhibitor and quantitation of metabolically generated cyanide. Journal of Pharmaceutical and Biomedical Analysis **39:** 1014-1020.

Lopez-Martin, M.C., Becana, M., Romero, L.C., Gotor, C. (2008). Knocking Out Cytosolic Cysteine Synthesis Compromises the Antioxidant Capacity of the Cytosol to Maintain Discrete Concentrations of Hydrogen Peroxide in Arabidopsis. Plant Physiol **147:** 562-572.

Lorrain, S., Vailleau, F., Balague, C., Roby, D. (2003). Lesion mimic mutants: keys for deciphering cell death and defense pathways in plants? Trends Plant Sci **8:** 263-271.

Lozano-Duran, R., Rosas-Diaz, T., Gusmaroli, G., Luna, A.P., Taconnat, L., Deng, X.W., Bejarano, E.R. (2011). Geminiviruses subvert ubiquitination by altering CSN-mediated derubylation of SCF E3 ligase complexes and inhibit jasmonate signaling in Arabidopsis thaliana. Plant Cell **23:** 1014-1032.

Mackenzie, S., McIntosh, L. (1999). Higher plant mitochondria. Plant Cell **11:** 571-586.

Millenaar, F.F., Lambers, H. (2003). The alternative oxidase: in vivo regulation and function. Plant Biol **5:** 2-15.

Miller, J.M., Conn, E.E. (1980). Metabolism of hydrogen cyanide by higher plants. Plant Physiol **65:** 1199-1202.

Mindrinos, M., Katagiri, F., Yu, G.L., Ausubel, F.M. (1994). The A. thaliana disease resistance gene RPS2 encodes a protein containing a nucleotide-binding site and leucine-rich repeats. Cell **78:** 1089-1099.

Mur, L.A., Laarhoven, L.J., Harren, F.J., Hall, M.A., Smith, A.R. (2008). Nitric oxide interacts with salicylate to regulate biphasic ethylene production during the hypersensitive response. Plant Physiol **148:** 1537-1546.

Murphy, A.M., Gilliland, A., York, C.J., Hyman, B., Carr, J.P. (2004). High-level expression of alternative oxidase protein sequences enhances the spread of viral vectors in resistant and susceptible plants. J Gen Virol **85:** 3777-3786.

Pandey, S.P., Somssich, I.E. (2009). The role of WRKY transcription factors in plant immunity. Plant Physiol **150:** 1648-1655.

Pieterse, C.M., Leon-Reyes, A., Van der Ent, S., Van Wees, S.C. (2009). Networking by small-molecule hormones in plant immunity. Nat Chem Biol **5:** 308-316.

Pieterse, C.M., van Wees, S.C., van Pelt, J.A., Knoester, M., Laan, R., Gerrits, H., Weisbeek, P.J., van Loon, L.C. (1998). A novel signaling pathway controlling induced systemic resistance in Arabidopsis. Plant Cell **10:** 1571-1580.

Piotrowski, M. (2008). Primary or secondary? Versatile nitrilases in plant metabolism. Phytochemistry **69:** 2655-2667.

Poulton, J.E. (1990). Cyanogenesis in Plants. Plant Physiol **94:** 401-405.

Reiner, A., Yekutieli, D., Benjamini, Y. (2003). Identifying differentially expressed genes using false discovery rate controlling procedures. Bioinformatics **19:** 368-375.

Rojas, M.R., Hagen, C., Lucas, W.J., Gilbertson, R.L. (2005). Exploiting chinks in the plant's armor: evolution and emergence of geminiviruses. Annu Rev Phytopathol **43:** 361-394.

Schneider, K., Mathur, J., Boudonck, K., Wells, B., Dolan, L., Roberts, K. (1998). The ROOT HAIRLESS 1 gene encodes a nuclear protein required for root hair initiation in Arabidopsis. Genes Dev **12:** 2013-2021.

Seo, S., Mitsuhara, I., Feng, J., Iwai, T., Hasegawa, M., Ohashi, Y. (2011). Cyanide, a coproduct of plant hormone ethylene biosynthesis, contributes to the resistance of rice to blast fungus. Plant Physiol **155:** 502-514.

Siegien, I., Bogatek, R. (2006). Cyanide action in plants - from toxic to regulatory. Acta Physiologiae Plantarum **28:** 483-497.

Spoel, S.H., Dong, X. (2008). Making sense of hormone crosstalk during plant immune responses. Cell Host Microbe **3:** 348-351.

Stelmaszynska, T. (1986). Formation of HCN and its chlorination to ClCN by stimulated human neutrophils--2. Oxidation of thiocyanate as a source of HCN. Int J Biochem **18:** 1107-1114.

Swanson, J., Kearney, B., Dahlbeck, D., Staskawicz, B.J. (1998). Cloned avirulence gene of *Xanthomonas campestris* pv. *vesicatoria* complements spontaneous race change mutant. Mol Plant–Microbe Interact **1:** 5–9.

Tornero, P., Dangl, J.L. (2001). A high-throughput method for quantifying growth of phytopathogenic bacteria in Arabidopsis thaliana. Plant J **28:** 475-481.

Toufighi, K., Brady, S.M., Austin, R., Ly, E., Provart, N.J. (2005). The Botany Array Resource: e-Northerns, Expression Angling, and promoter analyses. Plant J **43:** 153-163.

Tudzynski, B., Liu, S., Kelly, J.M. (2000). Carbon catabolite repression in plant pathogenic fungi: isolation and characterization of the Gibberella fujikuroi and Botrytis cinerea creA genes. FEMS Microbiol Lett **184:** 9-15.

van Loon, L.C., Geraats, B.P., Linthorst, H.J. (2006). Ethylene as a modulator of disease resistance in plants. Trends Plant Sci **11:** 184-191.

Vanlerberghe, G.C., McIntosh, L. (1997). ALTERNATIVE OXIDASE: From Gene to Function. Annu Rev Plant Physiol Plant Mol Biol **48:** 703-734.

Vlot, A.C., Klessig, D.F., Park, S.W. (2008). Systemic acquired resistance: the elusive signal(s). Curr Opin Plant Biol **11:** 436-442.

Wang, K.L.C., Li, H., Ecker, J.R. (2002). Ethylene biosynthesis and signaling networks. Plant Cell **14:** S131-S151.

Watanabe, M., Kusano, M., Oikawa, A., Fukushima, A., Noji, M., Saito, K. (2008). Physiological roles of the beta-substituted alanine synthase gene family in Arabidopsis. Plant Physiol **146:** 310-320.

Wettenhall, J.M., Simpson, K.M., Satterley, K., Smyth, G.K. (2006). affylmGUI: a graphical user interface for linear modeling of single channel microarray data. Bioinformatics **22:** 897-899.

Wong, C.E., Carson, R.A., Carr, J.P. (2002). Chemically induced virus resistance in Arabidopsis thaliana is independent of pathogenesis-related protein expression and the NPR1 gene. Mol Plant Microbe Interact **15:** 75-81.

Xu, X., Chen, C., Fan, B., Chen, Z. (2006). Physical and functional interactions between pathogen-induced Arabidopsis WRKY18, WRKY40, and WRKY60 transcription factors. Plant Cell **18:** 1310-1326.

Zagrobelny, M., Bak, S., Moller, B.L. (2008). Cyanogenesis in plants and arthropods. Phytochemistry.

Zheng, Z., Qamar, S.A., Chen, Z., Mengiste, T. (2006). Arabidopsis WRKY33 transcription factor is required for resistance to necrotrophic fungal pathogens. Plant J **48:** 592-605.

FIG. 1

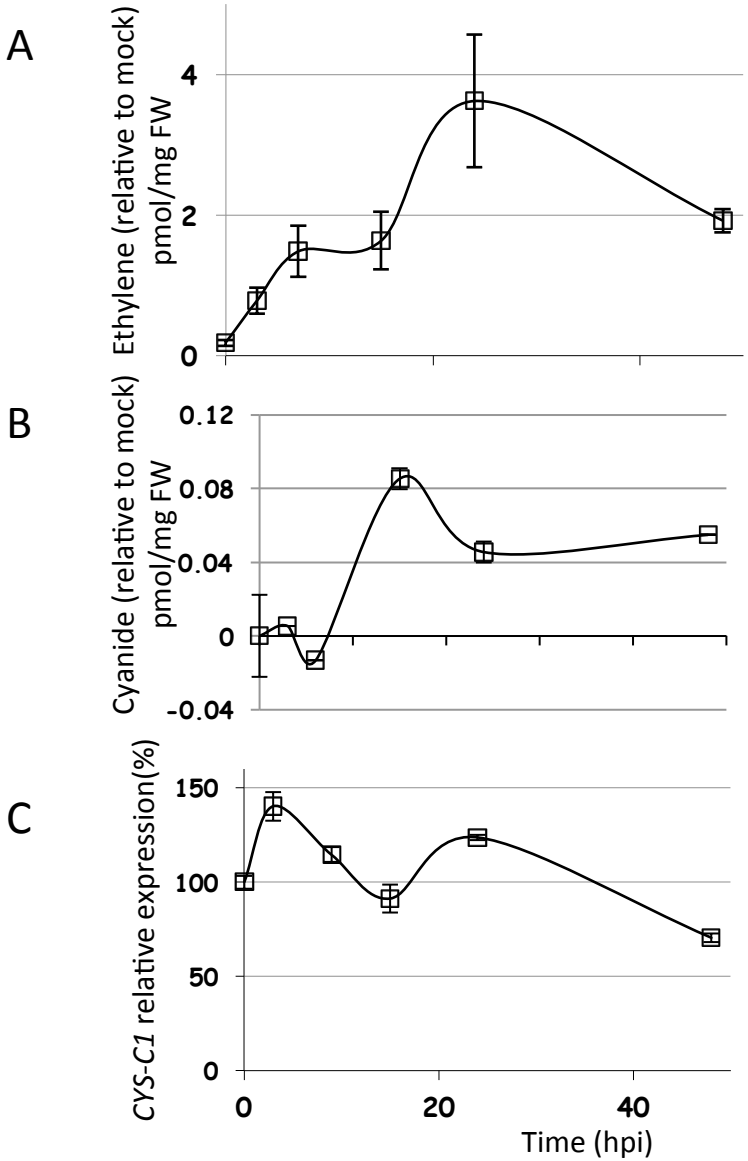

Figure 1. Time-course of the accumulation of ethylene (A) and cyanide (B) and the regulation of *CYS-C1* transcript (C) during the *A. thaliana-B. cinerea* interaction. Ethylene (A) and cyanide (B) were measured in leaf extracts of wild type plants grown for 6 to 7 weeks and infected with a spore suspension of *B. cinerea*. The results presented here are expressed as the mean ± standard deviation (SD) of a representative experiment in which 12-14 leaves from infected plants were pooled and three independent extractions were made from the pooled material. The experiment was repeated three times, with similar results obtained each time. The expression level of *CYS-C1* (C) was analyzed by real-time RT-PCR and referred to the *UBQ10* internal control. The data correspond to the means ± SD of three independent analyses using material grown in different batches at different times. For each analysis, 5-6 plants were pooled, and three independent RNA extractions were made from the pooled material. Two experimental replicates were made for each sample. The cyanide and *CYS-C1* expression values were normalized against the data obtained from plants treated with a mock solution. hpi, hours post-infection. Not-normalized data are shown in Supplemental Fig. 7A, 8A and 9A

FIG. 2

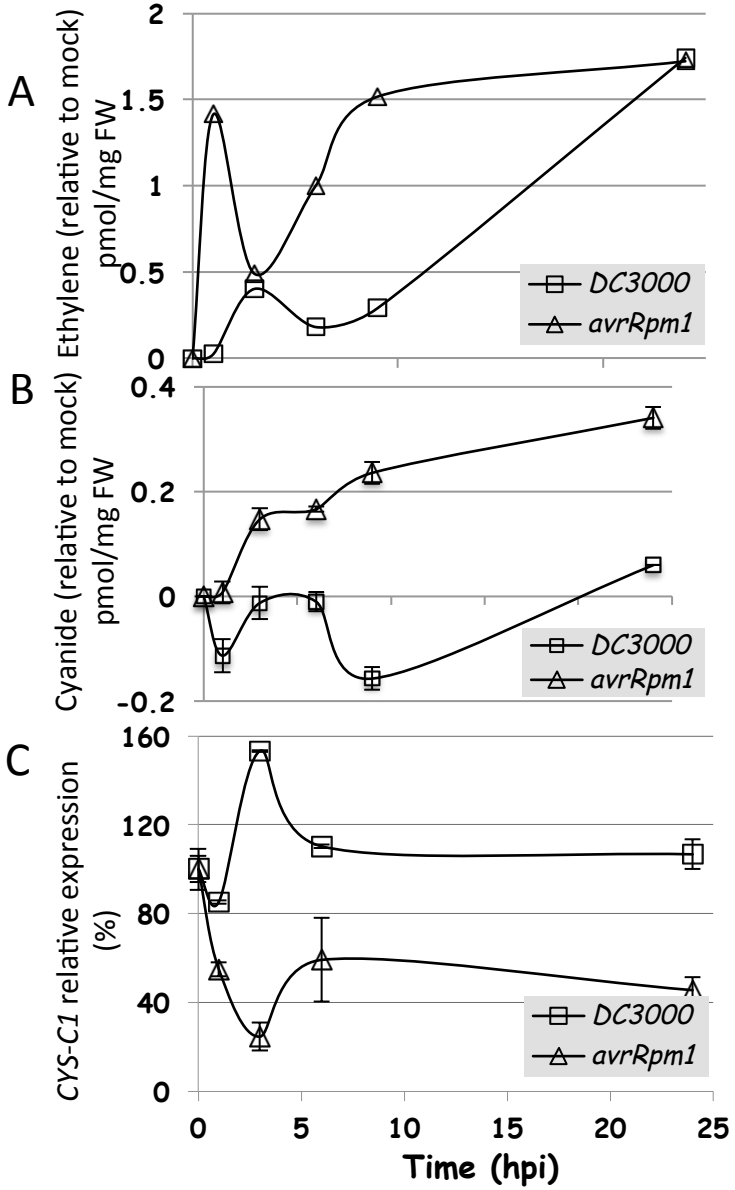

Figure 2. Time-course of the accumulation of ethylene (A) and cyanide (B) and the regulation of *CYS-C1* transcript (C) during the *A. thaliana-P. syringae* interactions. Ethylene (A) and cyanide (B) were measured in leaf extracts of wild type plants grown for 6 to 7 weeks and infected with a bacterial suspension of either *Pst DC3000* or *Pst DC3000 avrRpm1* as described in the Material and Methods. The results presented here are expressed as the mean ± SD of a representative experiment in which 12-14 leaves from infected plants were pooled and three independent extractions were made from the pooled material. The experiment was repeated three times, with similar results obtained each time. The expression level of *CYS-C1* (C) was analyzed by real-time RT-PCR and referred to the *UBQ10* internal control. The data correspond to the means ± SD of three independent analysis using material grown in different batches at different times. For each analysis, 5-6 plants were pooled, and three independent RNA extractions were made from the pooled material. Moreover, two experimental replicates were made for each sample. The data were normalized against the data obtained from plants treated with a mock solution. hpi, hours post-infection. Not-normalized data are shown in Supplemental Fig. S7B, S8B and S9B

FIG. 3

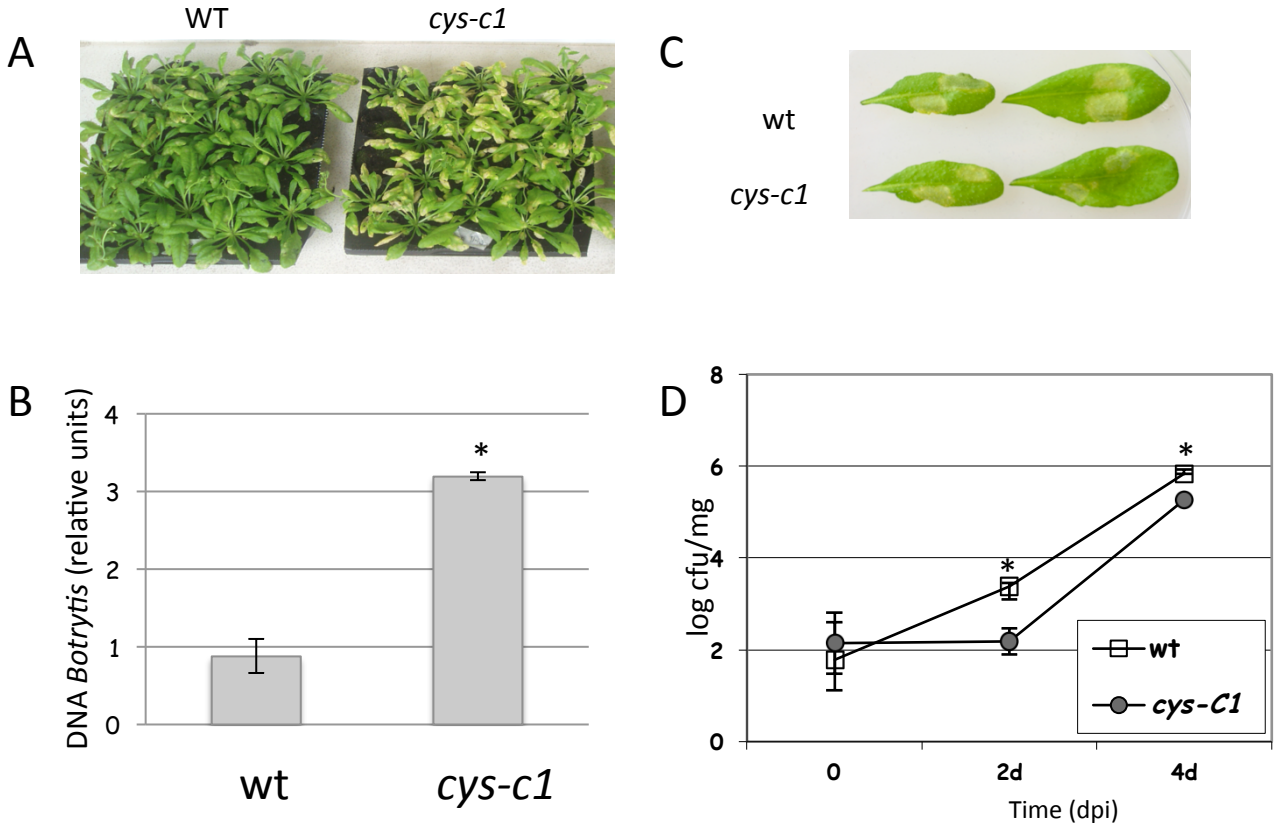

Figure 3. Responses of the *cys-c1* mutant to pathogen infection. A, B, Susceptibility of wild type and *cys-c1* mutant to *Botrytis cinerea* infection. A. Wild type and *cys-c1* mutant plants after 5 days of *B. cinerea* infection. B. Quantification of fungus growth was performed by real-time-PCR amplification of the *B. cinerea creA* gene, which was normalized against the Arabidopsis *UBQ10* gene. DNA was isolated from leaves 5 days after spore inoculation of 6- to 7-week-old wild type, mutant and complemented plants grown in parallel. The data correspond to the mean ± standard deviation (SD) of at least three independent analysis made from material grown in different batches at different times. For each analysis, twenty infected plants were pooled, and six independent DNA extractions were made from the pooled material. Moreover, two experimental replicates were made from each sample. C, D, Susceptibility of wild type and *cys-c1* mutants to infection with virulent *Pst DC3000* bacteria. C. Wild type and *cys-c1* mutant leaves after 3 days of *Pst DC3000* infection. D. Colony-forming units (cfu) were counted at 0, 2 and 4 days post-infection (dpi) of 6- to 7-week-old wild type and mutant plants grown in parallel. At total of 12 to 14 leaves were pooled for each analysis, in which three independent counts were made from the pooled material and two experimental replicates were made from each sample. The data correspond to the mean ± standard deviation (SD) of one representative experiment. *, $P<0.05$. The experiment was performed three times with material grown in different batches at different times; similar results were obtained for each iteration.

FIG. 4

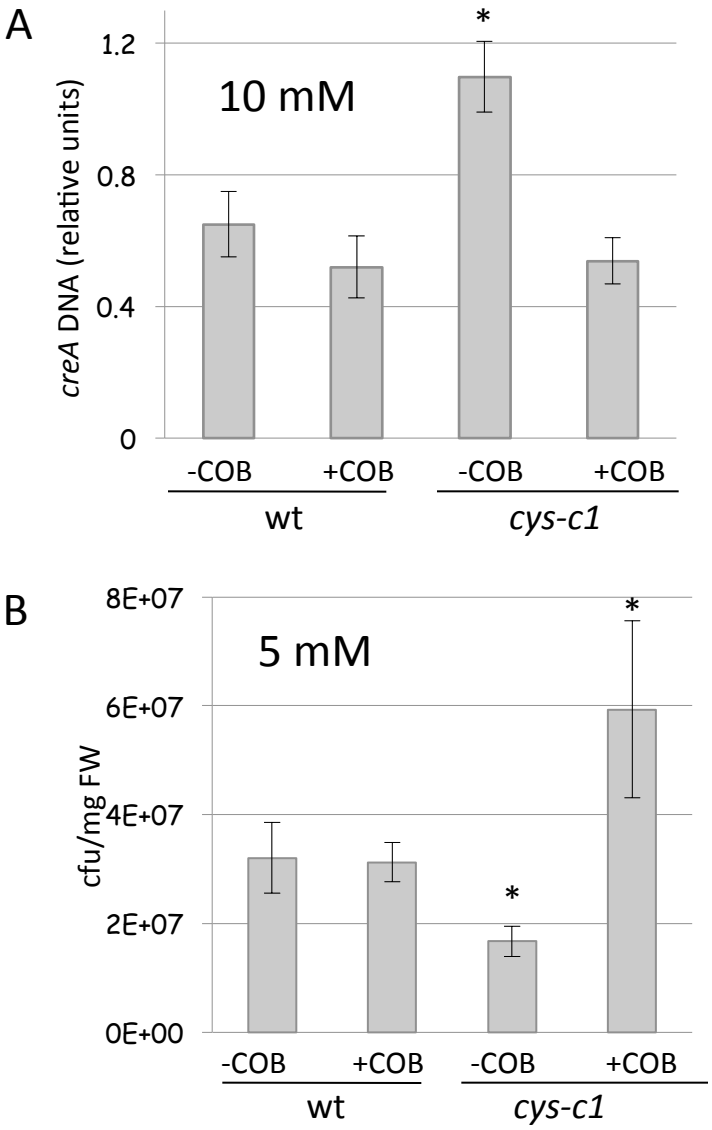

Figure 4. Hydroxocobalamin effect on plant susceptibility to pathogens. Wild type and *cys-c1* mutant plants were infected with *B. cinerea* (A) or *Pst DC3000* (B), as indicated in the Material and Methods and in Figures 3 and 4. Pathogens were collected in suspensions containing (+COB) or not containing (-COB) hydroxocobalamin at the concentration indicated and used to perform the susceptibility assays. Quantification of fungus growth was performed by real-time-PCR amplification of the *B. cinerea creA* gene, which was normalized against the Arabidopsis *UBQ10* gene. DNA was isolated from leaves 5 days after spore inoculation of 6- to 7-week-old wild type, mutant and complemented plants grown in parallel. Colony-forming units (cfu) were counted at 3 days post-infection, with 12 to 14 leaves pooled for each analysis. Three independent determinations were made from the pooled material, and two experimental replicates were made from each sample. The data correspond to the mean ± standard deviation (SD) of one representative experiment. *, $P<0.05$

FIG. 5

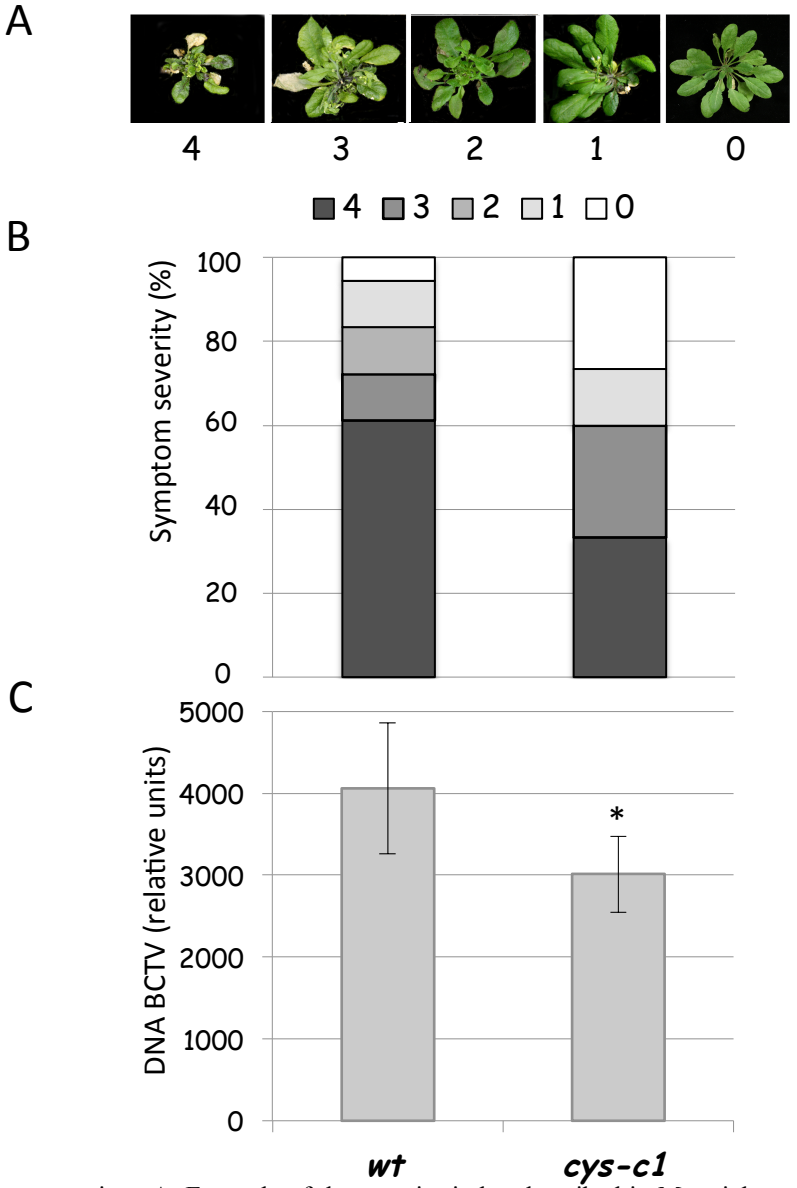

Figure 5. Response of the *cys-c1* mutant to virus. A, Example of the severity index described in Materials and Methods and Baliji *et al.* (2007). 0: no symptoms; 1 to 4, increasing severity of symptoms. B, Susceptibility of wild type and *cys-c1* mutant to BCTV infection. Whole six- to seven-week-old plants of each genotype were agroinoculated, and the symptom severity was recorded at 28 dpi. C, Quantification of virus growth was performed in the same plants at 28 dpi by real-time PCR amplification of the viral DNA, which was normalized against the Arabidopsis *UBQ10* gene. The data correspond to the mean ± standard deviation (SD) of three independent analyses made from material grown in different batches at different times. For each analysis, at least ten infected plants were pooled, and six independent DNA extractions were made from the pooled material. Two experimental replicates were performed from each sample. *, $P<0.05$

FIG. 6

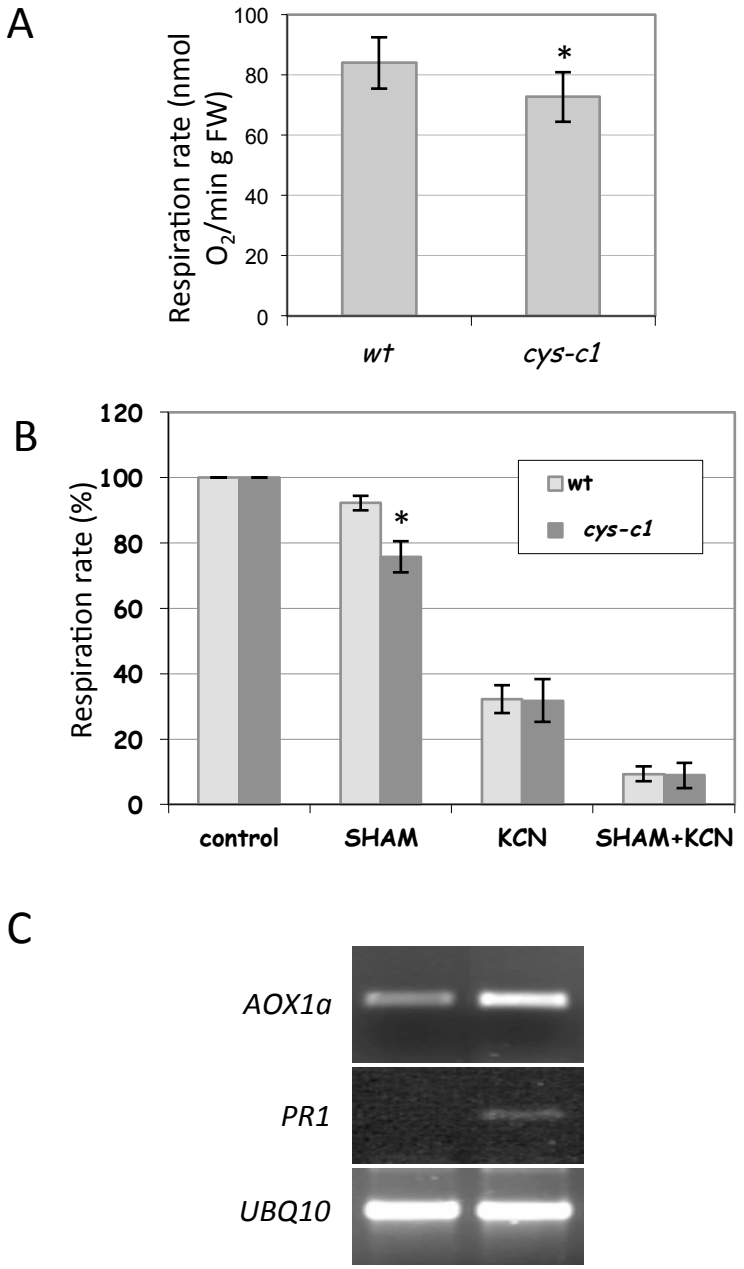

Figure 6. Respiration rates (A, B) and *AOXa1* and *PR1* expression levels (C) in leaves of wild type and *cys-c1* mutant plants. Cyanide-independent and alternative oxidase respiration were determined in the presence of 0.5 mM KCN or 4 mM SHAM, respectively. The transcription level of the alternative oxidase gene *AOXa1, PR1* and the control *UBQ10* was determined by RT-PCR in leaves of non infected 6- to 7-week-old plants. The data correspond to the mean ± standard deviation (SD) of at least three independent analysis made from material grown in different batches at different times. *, $P<0.05$.

FIG. 7

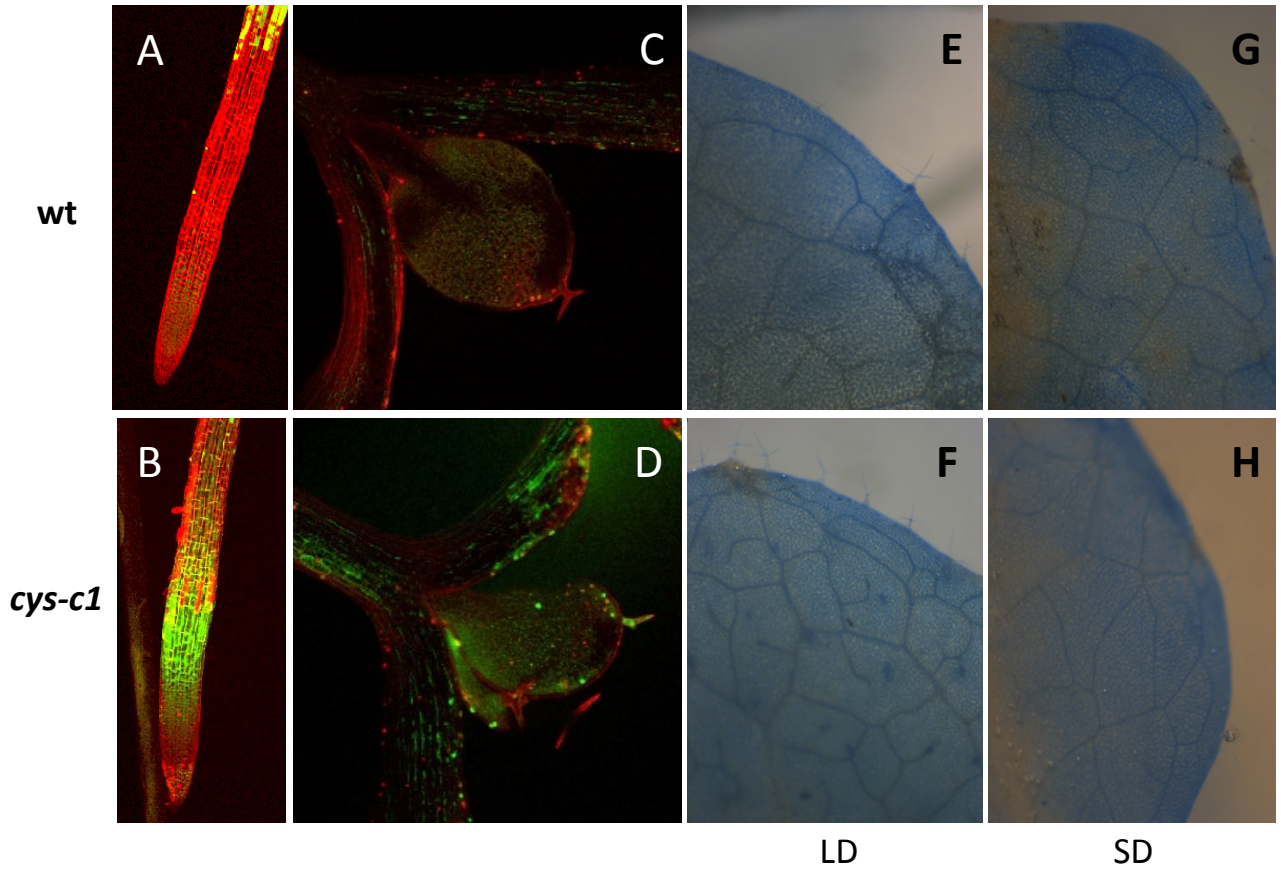

Figure 7. Accumulation of H_2O_2 and lesion formation in the *cys-c1* mutant. H_2O_2 was detected by H_2DCFDA staining in root (A-B) and cotyledons (C-D) from five-days-old wild type and *cys-c1* mutant plants cultured in MS medium. Lactophenol trypan blue was used to stain spontaneous cell death lesions (E-H). Detached leaves of plants grown in soil for three weeks in long-day conditions (E-F) or 6-7 weeks in short-day conditions (G-H) were used for the assay. All the experiments were repeated at least three times, with similar results obtained each time.